

Responses to Anonymous Referee #1

We greatly appreciated the reviewer for the insight comments and suggestions for improving the manuscript quality. Below, we have addressed your concerns and provided our point-by-point responses in blue.

General

This is an interesting study on 'trace elements', i.e., in my understanding metals, in aerosol particles sampled at Mt. Lushan in southern China in summer 2011 and spring 2012.

The measurements are interesting with regard to the implications of cloud processing and because the studied metals are tracers for a variety of sources.

The back trajectory and source contribution modelling in the papers shines light on the origin of different families of metals.

I wonder how it can be better evidenced that the aerosol particles sampled in Guniubei have really been cloud-processed? As of now, it seems that this is Observation based, in that if there was a cloud at Mt. Lushan, the sampled particles were assigned as 'cloud-processed'. Is there an objective way to flag samples that they must have been cloud-processed?

In field observation, it is very difficult to prove if the aerosol particles have been cloud-processed at once when there are no occurring clouds at the sampling site. However, we can hardly neglect the effect of cloud processing on particles during transport in the air on account of the widespread cloud covering about 60% of the earth surface. By far, the impacts of cloud processing on aerosols are mostly investigated by laboratory simulations. In this study, as mentioned in Section 3.4.4, we collected the aerosols for several hours immediately after the disappearance of the cloud and marked the samples as cloud-processed. In truth, the cloud events were fairly evident to be distinguished and the sampling intervals were short enough to minimize the outside interference to the cloud-processed aerosols. Real-time meteorology parameters such

as wind speed (WS), relative humidity (RH) and visibility were additionally used to support the identification of cloud process. For instance, Figure R1-1 displays the ambient circumstances of non-precipitation cloud process on 18 April 2012 with averaged $WS < 1.0 \text{ m s}^{-1}$, $RH \geq 99\%$ and $Visibility < 0.05 \text{ km}$ (Table R1-1), adequately indicating the actual cloud-processing. Figure R1-2 (a) and (b) shows the typical circumstances of a developing/coming cloud and a disappearing/leaving cloud, presenting a much better $Visibility > 2 \text{ km}$. Moreover, the cloud-processed particles were commonly found to exhibit a much thicker aqueous layer covering them through TEM analysis. All in all, we can well recognize and flag the cloud-processed samples by timely artificial observation of cloud events and experienced manual sampling of post-cloud particles with short time intervals.

Another detailed map of the orography of the site, i.e., the mountain, the sampling place and key meteorology parameters would also be of assistance to the reader. Maybe some supplementary material can be used for this.

It is a very considerate suggestion. We have added another more detailed topographical map of Mt. Lushan and the sampling site as the supplementary material. The key meteorology parameters such as temperature (T), relative humidity (RH), wind speed (WS) and Visibility are listed in Table R1-1 and will also be added into the supplement. Generally, it can be seen that the summer days exhibited higher temperature, RH and wind speed than spring. The relatively high RH were likely to be contributed by the frequent cloud and rainfall at Mt. Lushan. Obviously, the two selected typical cloud events were characterized by extremely high RH and much low wind speed along with a visibility of nearly 0 km.

Overall, this is a very nice and thoughtful contribution which merits publication in ACPD subject to minor revision.

Thank you very much!

Details

Page 13003, line 4: Atmospheric lifetime of particles should not be much beyond 10

days, cf Jaenicke (1978), pls reconsider the statement of ‘weeks’

We have deleted the statements of “weeks” with caution in the revised manuscript, as particles with sizes larger than 1 μm usually have short residence time in the troposphere.

Table R1-1. Key meteorology parameters (Mean \pm SD) during summer of 2011 and spring of 2012, as well as during the two selected cloud events on 11 September 2011 and 18 April 2012. Note that the statistical meteorology parameters for summer of 2011 and spring of 2012 were computed including rainy-days and cloudy-days.

Periods	T ($^{\circ}\text{C}$)	RH (%)	WS (m s^{-1})	Visibility (km)
Summer, 2011	20.0 ± 4.5	88 ± 12	12.7 ± 9.4	11.6 ± 7.7
Spring, 2012	13.6 ± 4.3	76 ± 26	3.6 ± 2.8	10.7 ± 8.1
11 September 2011	20.7 ± 0.4	99	1.7 ± 3.8	0
18 April 2012	13.3 ± 0.9	99	0.5 ± 0.5	0



Figure R1-1. The thick cloud/fog on 18 April 2012 around the cloud water sampler.

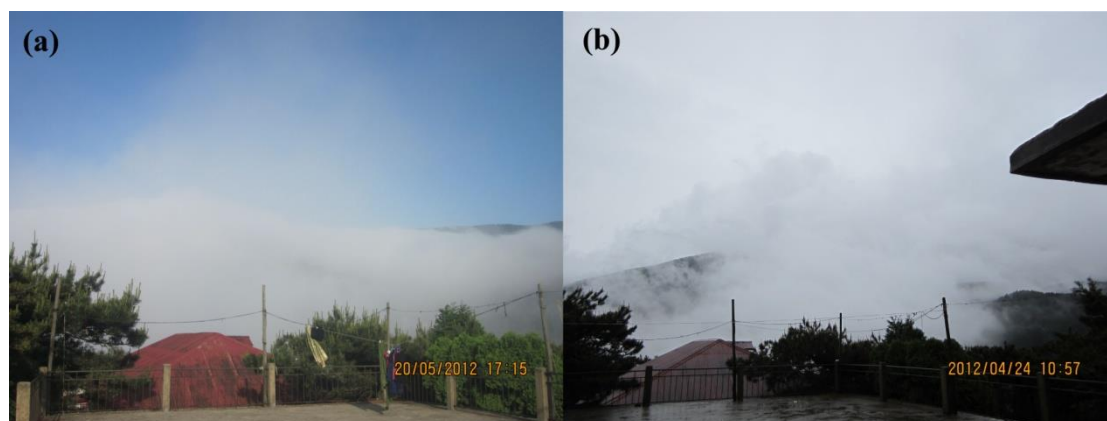


Figure R1-2. Scenes before (a) and after (b) cloud events observed at the sampling site.

Responses to Anonymous Referee #2

We greatly appreciated the reviewer for the insight comments and suggestions for improving the quality of this manuscript. Below, we have addressed your concerns and provided our point-by-point responses in blue.

This study provides various information on the concentrations and solubilities of many metal ions in the atmosphere around Mt. Lushan, southern China. Since air pollution in China has been an important issue which can affect air quality not only in China, but also in other parts in East Asia due to the long-range transport. Thus, I think that this study is worth publishing to reveal information of the metal ions in fine particulate matters in the atmosphere in East Asia.

2.2. Sample collection: More details of the sampling of the cloud residues must be described.

The sampling system of the cloud residues was initially used at Mt. Tai in 2010 (Li et al., 2011). As shown in Figure R2-1, the moisture of the cloud droplets is removed by a diffusion dryer filled with desiccant (silica gel) to prevent the impact of the water vapor on TEM grids. Then, the individual residues are collected onto TEM grids using a

single-stage cascade impactor with a 0.5 mm diameter jet nozzle. The calculated effective size d_{50} for cloud droplet is about 0.7 μm and the collection efficiency is estimated to be 5-10%. In this study, a low sampling flow rate of 0.5 l min^{-1} and an optimum sampling time of about 12 min were employed, neither destroying the TEM grids nor overlapping each individual residues.

We have added the description of the sampling system of cloud residues into the supplement.

2.3.2 Water-soluble fraction: How can avoid precipitation of highly insoluble elements such as Fe^{3+} and Al^{3+} by extraction using pure water. If the pH is above 5, the soluble Fe^{3+} in water is less than 60ppb. Is it possible to keep ferric ion in the water and to avoid formation of iron precipitates in your samples?

Ultrapure water were used to extract water-soluble metal ions in atmospheric particles in many studies, representing the highly soluble/bioavailable fraction. The extraction method was improved based on a chemical speciation scheme of trace elements in fine particles (Fernández-Espinosa et al., 2004), which was interpreted in the responses to the editor comment in detail. Ultra-sonication was implemented to prevent the formation of precipitates by keeping the dissolving constituents of insoluble elements (such as Fe^{3+} and Al^{3+}) in colloidal state at neutral pH as much as possible during the extraction procedure. The filtered solution was immediately transferred into glass bottles and high pure hydrochloric acid was then added to adjust the pH to less than 1, transforming the colloidal metal back to dissolved state and lessening the adsorption by glass walls. Thus, we expect that the dissolved fraction (by water) of highly insoluble elements in aerosols were sufficiently extracted and determined.

Results and discussion: (1) The solubility of metal ions has been investigated in various studies. Thus, it is essential for the authors to compare their results with other published data. In particular, the difference of the protocol to extract metal ions among different studies must be reviewed to compare each result.

Comparison of aerosol element solubility in various studies was displayed in

supplement (Figure S5). No significant relationships were observed among these studies except the commonly low solubility for crustal elements such as Fe, Al and Cr. Accordingly, environment type, extraction method and analysis instrument are compared in Table R2-1. The major experimental differences are the type of environment and extraction method for total content of trace elements. The higher solubility for Mn, Cu and Fe at Mt. Lushan should be attributed to the frequent cloud events at high altitude. Larger aerosol size (TSP) and stronger acid mixture (HNO_3 -HF) were responsible for the various gap of solubility for Ba, Mo, Fe and Al in TSP over East China Sea and in $\text{PM}_{2.5}$ at Mt. Lushan. However, the differences of extraction method were not so much remarkable and the overall solubility trend for most elements were similar (decreasing from Zn to Cr) in each study, indicating the much less significance of extraction method than the type of environment in these studies. The water solubility estimated from this study is still meaningful to assess the bioavailability and mobility of aerosol trace elements. More important influencing factors were investigated in the manuscript.

We have added Table R2-1 and reviewed the differences of protocols and results among various studies in the supplement.

(2) The experiment for the cloud processing is interesting. However, please write more details about the experiment such as (i) how did you collect the cloud water and (ii) how did you prepare the cloud residue.

(i) Bulk cloud water samples were collected by the improved Caltech Active Strand Cloudwater Collector (CASCC2 (Demos et al., 1996)). The CASCC2 is a single-stage collector with a sampling flow rate of $24.5 \text{ m}^3 \text{ min}^{-1}$. Air with cloud droplets are inhaled into the instrument and impacted on vertical $508 \text{ }\mu\text{m}$ diameter Teflon strands. The droplets are then collected into a Teflon sample trough along the strands and flows into a 500 ml high-density polyethylene bottle. The theoretical sampling efficiency for size cut of $3.5 \text{ }\mu\text{m}$ droplet diameter corresponds to 50%. In this study, the sampling interval of cloud water was 2 to 3 hours. Filtered cloud water ($\sim 30 \text{ ml}$) were immediately stored in brown glass bottles at $4 \text{ }^\circ\text{C}$ with preservation of 1% v/v high pure hydrochloric acid.

We have added the sampling of cloud water into Section 2.2 of the revised manuscript and into the supplement.

(ii) The sampling process is described above. Copper TEM grids coated with carbon film were placed in the impactor to collect individual cloud residues. An optical microscopy with magnification from $\times 500$ to $\times 1200$ was immediately used to check whether the carbon film and particle distribution on the TEM grid were suitable for analysis. If suitable, the grid would be placed in a sealed, dry plastic tube and stored in a desiccator at 25 °C and $20 \pm 3\%$ RH until the laboratory TEM/EDS analysis. Otherwise, another satisfactory sample shall be collected and preserved.

We have described the more detailed preparation of cloud residues in the revised manuscript.

(3) This study suggests that Ba is of metallurgical smelting origin. What kind of smelting activity can be suggested as a source of Ba.

Ba is a widely distributed alkaline-earth metal that primarily exists in barite (BaSO_4) and witherite (BaCO_3). In most case, Ba is clustered with Al, Fe and Ca, which indicates a source of crust or soil. However, we found Ba had relatively high EF values (>10) and was clustered with As and Cr at Mt. Lushan. Table S2 also showed an obviously higher concentration of Ba at Mt. Lushan than the other mountains and Shanghai, suggesting the anthropogenic pollution of Ba. Furthermore, Figure 6(k) identified southeastern Hunan and central Jiangxi as the most potential source regions. Since there are abundant mineral resources such as barite and realgar in Hunan province which is the most important production and export base of mineral products in China, the vast opencast mining of barite is considered to be the primary source of fine particle Ba at Mt. Lushan.

P.13010, L1: “contributed the highest” should be “contributed to the highest”.

It has been changed in the revised manuscript.

P.13012, L1: “applied to identify” should be “applied to identification of”.

It has been changed in the revised manuscript.

P.13017, L13: “That” should be “This result”.

It has been changed in the revised manuscript.

P.13017, L22: “contributed the” should be “contributed to the”.

It has been changed in the revised manuscript.

Fig. 2: Unit must be shown for the vertical axis.

The unit of the vertical axis is ng m^{-3} . For concision and good-looking, the unit is added into the figure caption in the revised manuscript.

Table R2-1. Differences of environment type, extraction method and instrument in determining aerosol element solubility in various studies.

Location	Type of environment	Extraction method		Instrument	Ref
		Soluble	Total		
Mt. Lushan (PM _{2.5})	Rural mountain	Ultrapure water	HNO ₃ -H ₂ O ₂ , microwave digestion	ICP-MS	This study
East China Sea (TSP)	Sea surface	Milli-Q water	HNO ₃ -HF, microwave digestion	ICP-MS	(Hsu et al., 2010)
Edinburgh, UK (PM _{2.5})	Urban background	Ultrapure water	HNO ₃ -HCl, heating	ICP-MS	(Heal et al., 2005)
Nanjing, China (PM _{2.5})	Urban city	Glycine	HNO ₃ -H ₂ O ₂ , microwave digestion	ICP-OES & ICP-MS	(Hu et al., 2012)

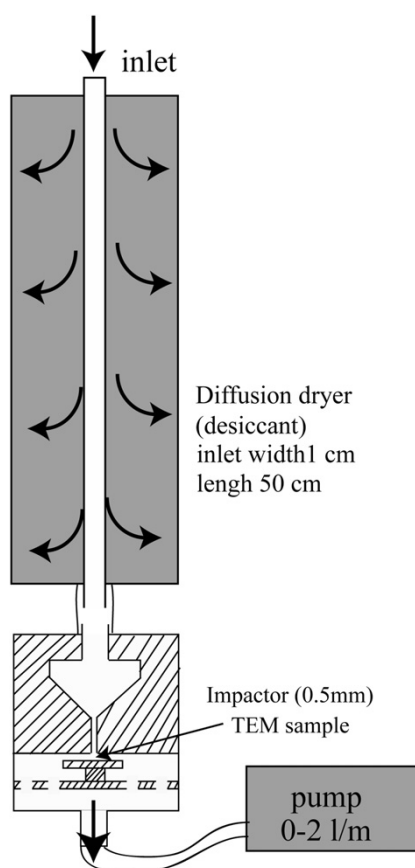


Figure R2-1. Schematic of the cloud droplet residues sampling system.

References:

- Demoz, B. B., Collett, J. L., Jr., and Daube, B. C., Jr.: On the Caltech active strand cloudwater collectors, *Atmos. Res.*, 41, 47-62, 10.1016/0169-8095(95)00044-5, 1996.
- Fernández-Espinosa, A. J., Rodríguez, M. T., and Álvarez, F. F.: Source characterisation of fine urban particles by multivariate analysis of trace metals speciation, *Atmos. Environ.*, 38, 873-886, 10.1016/j.atmosenv.2003.10.046, 2004.
- Heal, M. R., Hibbs, L. R., Agius, R. M., and Beverland, I. J.: Total and water-soluble trace metal content of urban background PM₁₀, PM_{2.5} and black smoke in Edinburgh, UK, *Atmos. Environ.*, 39, 1417-1430, doi:10.1016/j.atmosenv.2004.11.026, 2005.
- Hsu, S.-C., Wong, G. T. F., Gong, G.-C., Shiah, F.-K., Huang, Y.-T., Kao, S.-J., Tsai, F., Candice Lung, S.-C., Lin, F.-J., Lin, I. I., Hung, C.-C., and Tseng, C.-M.: Sources, solubility, and dry deposition of aerosol trace elements over the East China Sea, *Mar. Chem.*, 120, 116-127, doi:10.1016/j.marchem.2008.10.003, 2010.
- Hu, X., Zhang, Y., Ding, Z., Wang, T., Lian, H., Sun, Y., and Wu, J.: Bioaccessibility and health risk of arsenic and heavy metals (Cd, Co, Cr, Cu, Ni, Pb, Zn and Mn) in TSP and PM_{2.5} in Nanjing, China, *Atmos. Environ.*, 57, 146-152,

<http://dx.doi.org/10.1016/j.atmosenv.2012.04.056>, 2012.

Li, W., Li, P., Sun, G., Zhou, S., Yuan, Q., and Wang, W.: Cloud residues and interstitial aerosols from non-precipitating clouds over an industrial and urban area in northern China, *Atmospheric Environment*, 45, 2488-2495, [10.1016/j.atmosenv.2011.02.044](https://doi.org/10.1016/j.atmosenv.2011.02.044), 2011.

Responses to J. Ma (Editor)

We greatly appreciate the editor for taking time to read this manuscript and providing insight comments. Below, we have addressed your concerns and provided our point-by-point responses in blue.

Solubility refers to the extent to which a substance dissolves in a particular solvent. According to IUPAC definition, solubility is the composition of a saturated solution, expressed in terms of the proportion of a designated solute in a designated solvent (<http://goldbook.iupac.org/S05740.html>). The solubility of a substance fundamentally depends on the physical and chemical properties of the solute and solvent as well as on temperature, pressure and the pH of the solution (<http://en.wikipedia.org/wiki/Solubility>).

In this paper, Li et al. (2015) defines element solubility as the percentage of water-soluble concentrations of an element divided by its total concentration (Page 13018, Line 3-4). This definition has a conflict with the traditional concept of solubility in chemistry. The word “solubility” is used in the title of the paper, and appears frequently in the Abstract and the Introduction, but its own definition is not available until Sect. 3.4.

The definition of solubility in our study is indeed different from its traditional concept in chemistry defined by IUPAC and Wikipedia. Apart from the total content of trace elements, we also determined the concentration of their water-soluble fraction which are highly reactive in aqueous phase of aerosols and can bring great damage to human health and ecosystem due to their high mobility and bioavailability.

Solubility is usually calculated as the ratio of dissolved trace metal concentration to total concentration in work on aerosol dissolution (Deguillaume et al., 2005). The solubility here represents the capacity of an element's chemical reactivity/mobility as well as the degree of its bioavailability. In this study, the solubility concept, defined as the percentage of water-soluble concentrations of an element divided by its total concentration, was modified from sequential extraction procedures for trace metals speciation (see the next responses for detail).

In order to avoid misunderstanding and to distinguish from traditional concept of solubility, we have shifted forward our definition of solubility into the Introduction.

The authors also use the phrase "total fraction" to describe the total concentration of trace elements in fine particles. In addition to ionic compounds (water-soluble fraction) and elementary substances of trace elements, are there any other forms of elements existing in the total fraction which were experimentally analyzed in this study? Again, "element solubility" in this study appears to have nothing to do either with the solubility of ionic compounds or the solubility of elementary substances.

The phrase "total fraction" here means the total content of water soluble and water insoluble fraction of trace elements. Tessier et al. (1979) developed a sequential extraction procedure for partitioning the speciation of particulate trace metals, including *Water soluble + Exchangeable, Bound to carbonates, Bound to Fe-Mn oxides, Bound to organic matter, and Residual* fraction. Fernández-Espinosa et al. (2004) divided chemical speciation of trace metals in fine particles into four metallic fractions: *Soluble and exchangeable metals; Carbonates, oxides and reducible metals; Bound to organic matter, oxidisable and sulphidic metals; and Residual metals*. As we primarily focused on the bioavailability (water solubility) and total concentration of trace elements, extraction procedure in this work concentrated on the aqueous extraction (simulating the dissolution of soluble fraction of aerosol elements) and the acid extraction (approximating the total content of aerosol elements), regardless of the other partitioned speciation. The element solubility defined in this study was accordingly derived from the modified extraction procedure.

It is worth noting that the above partitioning method for trace elements speciation using sequential extraction procedure is based upon their likely released fraction under various simulated environmental conditions, rather than the specific chemical forms like ionic compounds or elementary substances, etc.

Reference

Li, T., Wang, Y., Li, W. J., Chen, J. M., Wang, T., and Wang, W. X.: Concentrations and solubility of trace elements in fine particles at a mountain site, southern China: regional sources and cloud processing, *Atmos. Chem. Phys. Discuss.*, 15, 13001-13042, 10.5194/acpd-15-13001-2015, 2015.

References:

- Deguillaume, L., Leriche, M., Desboeufs, K., Mailhot, G., George, C., and Chaumerliac†, N.: Transition metals in atmospheric liquid phases: Sources, reactivity, and sensitive parameters, *Chem. Rev.*, 105, 3388-3431, doi:10.1021/cr040649c, 2005.
- Fernández-Espinosa, A. J., Rodríguez, M. T., and Álvarez, F. F.: Source characterisation of fine urban particles by multivariate analysis of trace metals speciation, *Atmos. Environ.*, 38, 873-886, 10.1016/j.atmosenv.2003.10.046, 2004.
- Tessier, A., Campbell, P. G. C., and Bisson, M.: Sequential extraction procedure for the speciation of particulate trace metals, *Anal. Chem.*, 51, 844-851, 10.1021/ac50043a017, 1979.

Responses to Referee Anonymous (Short Comment)

We greatly appreciated R. Anonymous for providing comments and suggestions to this manuscript. Below, we have addressed your concerns and provided our point-by-point responses in blue.

It has been stated clearly in “Aims and scope” of this journal that “The journal scope is focused on studies with general implications for atmospheric science rather than investigations that are primarily of local or technical interest.” Apparently, this manuscript is a local interest in a single site of China.

We seriously considered your view of “Apparently, this manuscript is a local interest in

a single site of China”, which is the reason you state “This manuscript does not meet the scope of ACP”.

We carefully read the “Aims and scope” of ACP and make sure that our manuscript conforms fine to the scope of the journal. This manuscript is a research article subjected to field measurements of aerosols and clouds. We focused on the regional atmospheric pollution and the impact of the widespread cloud on aerosols in the acid rain area in southern China, rather than a local interest. The reasons we selected Mt. Lushan as the observation site is as follows:

1. Mt. Lushan, far from heavy industrial regions, is a representative regional atmosphere background station in southern China; the results would be helpful to evaluate the regional air quality.
2. The location and high altitude (1165 m a.s.l., near planetary boundary layer) of the observation site make it a favorable platform to study regional and long-range transport of atmospheric pollutants from Eastern and Southern coastal China such as Yangtze River delta (YRD) and Pearl River delta (PRD).
3. As cloud process makes significant contributions to the aerosol evolution/modification, the frequent cloud events at Mt. Lushan are in favor of investigating the impact of actual cloud processing on aerosols.

Finally, our results demonstrated the transport of regional air pollution and the important effect of cloud processing on aerosol properties, implying significant contributions of regional human activities, long-range transport and substantial cloud processing to air pollution and aerosol solubility in southern China or even in East Asia.

Overall, we consider that this manuscript accords well with the scope of ACP.

1 **Concentrations and solubility of trace elements in fine particles**
2 **at a mountain site, southern China: regional sources and cloud**
3 **processing**

4
5 **T. Li¹, Y. Wang¹, W. J. Li², J. M. Chen^{1, 2}, T. Wang³ and W. X. Wang²**

6 [1]{School of Environmental Science and Engineering, Shandong University, Jinan, Shandong
7 250100, China}

8 [2]{Environment Research Institute, Shandong University, Jinan, Shandong 250100, China}

9 [3]{Department of Civil and Environmental Engineering, the Hong Kong Polytechnic University,
10 Hong Kong, China}

11 Correspondence to: Y. Wang (wy@sdu.edu.cn)

12

13 **Abstract**

14 The concentrations and solubility of twelve trace elements in PM_{2.5} at Mt. Lushan, southern China,
15 were investigated during the summer of 2011 and the spring of 2012. The average PM_{2.5} mass was
16 $55.2 \pm 20.1 \mu\text{g m}^{-3}$ during the observation period. Temporal variations of all trace elements including
17 total and water-soluble fractions with several dust storm spikes for total fraction Al and Fe were
18 observed. The enrichment factor (EF) values were one order of magnitude higher for the
19 water-soluble fractions versus the total fractions of trace elements. Four major emission sources were
20 classified by principal component analysis (PCA), namely nonferrous metal mining and smelting (for
21 Cr, As, Ba and parts of Zn), coal combustion (for Pb, Zn, Se, Cu and Mn), crustal materials (for Al
22 and Fe) and municipal solid waste incineration (for Cd and Mo). Trajectory cluster analysis and the
23 potential source contribution function (PSCF) consistently identified the Yangtze River Delta (YRD),
24 the Pearl River Delta (PRD) and parts of Hunan and Jiangxi as the major source regions and
25 pathways for anthropogenic elements, while northern China was identified for crustal elements. In

1 contrast, the local Jiangxi area has become the most significant contributor to the solubility of most
2 trace elements, apart from the YRD with severe air pollution. In addition, the solubility alteration of
3 trace elements in cloud events was investigated and transmission electron microscopy (TEM)
4 analysis indicated that the irreversible alteration of particle morphology by cloud processing was
5 highly responsible for the enhancement of element solubility. Our work implies an important role of
6 regional anthropogenic pollution and cloud processing in the evolution of trace element solubility
7 during transport.

8 **1 Introduction**

9 Epidemiologic studies have associated long-term exposure to highly inhalable ambient fine
10 particulate matter ($\leq 2.5 \mu\text{m}$, $\text{PM}_{2.5}$) with many adverse health outcomes such as cardiovascular and
11 respiratory morbidity and mortality, whether in urban or rural areas (Hoek et al., 2013;Cao et al.,
12 2012;Weichenthal et al., 2014). Sustained exposure to high concentrations of PM air pollution has
13 been suggested to contribute to a decrease in life expectancy of approximately 3.0 y in China (Chen
14 et al., 2013). The long atmospheric lifetimes of days ~~or even weeks~~ give fine particles opportunities
15 to be subject to long-range transboundary or intercontinental transport in the air and to deposition
16 toward remote areas, carrying abundant anthropogenic pollutants and affecting ecosystems
17 (Mahowald, 2011). Fine particles are also responsible for regional and global climate change and the
18 hydrologic cycle interference through radiative forcing directly by reflecting sunlight and indirectly
19 by changing cloud properties and precipitation acting as cloud condensation nuclei (Kaufman et al.,
20 2002).

21 Although trace elements constitute only a small proportion of fine particle mass, their negative
22 impacts on human health and ecosystems have attracted considerable attention because of their
23 toxicity and bioaccumulation by inhalation and deposition. Toxicological and epidemiologic studies
24 often suggest trace metals, particularly water-soluble metals which are more easily bioavailable, as
25 the critical components harmful to the cardiopulmonary system through oxidative chemistry
26 (Cakmak et al., 2014;Costa and Dreher, 1997). Soluble trace elements, especially the transition
27 metals, are likely to be the primary drivers of the generation of reactive oxygen species, inducing
28 cellular inflammation (Charrier et al., 2014;Cheung et al., 2012;Shafer et al., 2010). Besides, trace

Comment [It1]: Deleted

1 metal ions also play an important catalysis role in secondary aqueous-phase (Harris et al., 2013) and
2 particle-phase (Clements et al., 2013) sulphate formation, heterogeneous production and elimination
3 of gas-phase hydrogen peroxide (Guo et al., 2014a) as well as multiphase cloud chemistry
4 (Deguillaume et al., 2004). Importantly, most anthropogenic trace elements in ambient air are
5 considered to be mainly concentrated on fine particles, strengthening their toxicity. Therefore,
6 understanding both the concentrations and water solubility of fine particle trace elements is essential
7 for revealing their bioavailability in ambient environments and reactivity in atmospheric chemistry.
8 Diverse characteristics and sources of atmospheric trace elements have been investigated in various
9 areas. For example, regional background, urban and industrial sites in Spain were found to have
10 clearly different concentration levels and source origins of trace elements in PM (Querol et al., 2007);
11 technogenic metalliferous fine aerosols observed in urban Montseny demonstrated the
12 spatiotemporal variability of trace metal pollution (Moreno et al., 2011); traffic, static combustion
13 and crustal were suggested as the main sources for Fe, Zn, Pb and Cu in PM_{2.5} in an urban
14 background area in Edinburgh (Heal et al., 2005); meanwhile, stationary industrial emissions from
15 coal combustion were confirmed as the contributor to substantial atmospheric lead pollution of PM_{2.5}
16 in Shanghai (Chen et al., 2008). The United States has already established a spatially gridded
17 national emissions inventory of PM_{2.5} trace elements in speciation profiles with the dominant sources
18 of crustal, biomass burning, coal combustion and industrial processing (Reff. et al., 2009). In Asia,
19 atmospheric metallic element pollution by human activities has been surveyed, with the highest
20 metal concentrations occurring in China (Fang et al., 2010). Coal combustion, nonferrous metal
21 smelting and iron and steel manufacturing are found to be the major disproportionate sources of
22 atmospheric hazardous trace elements in China according to the latest anthropogenic emissions
23 inventory, which highlighted an increasing trend in air pollution by toxic heavy metals (Cheng et al.,
24 2015).
25 Recently, many field observations have found that even remote mountains and oceans have been
26 polluted by anthropogenic trace elements in fine particles, significantly confirming the contributions
27 of long-range transport (Deng et al., 2011; Schwab, 2004; Fomba et al., 2013). A few studies on dust
28 in Asia (Takahashi et al., 2011; Hsu et al., 2013) indicate that the water solubility of trace elements

1 could be modified during long-range transport, probably affected by emission sources, anthropogenic
2 pollution, acid processing and photochemical aging, etc. (Hsu et al., 2010). However, little
3 information about fine particle trace elements has been reported with regard to the identification of
4 source regions or pathways, and the main mechanism of trace element dissolution by atmospheric
5 processing is still unclear.

6 This paper provides a dataset of the concentration and solubility (defined as the proportion of
7 dissolved element concentration in total content) ~~levels~~ of trace elements in fine particles at Mt.
8 Lushan, a high, rural mountain within an acid precipitation area in southern China. We focused on
9 identifying the potential source region distributions for individual elements, aiming to evaluate the
10 contributions of local, regional and long-range transport. Regional contributions to element solubility
11 were also preliminarily investigated. One condensation-evaporation cloud cycle can increase aerosol
12 solubility, and atmospheric aerosols may experience up to ten cloud cycles before removal
13 (Desboeufs et al., 2001; Spokes et al., 1994); hence, we intensively discussed the influence of actual
14 cloud processing on the alteration of fine particle trace element solubility, considering the rather
15 frequent cloud events at Mt. Lushan. The size, mixing state and chemical composition of individual
16 metal particles in cloud residues were detected using transmission electron microscopy (TEM) to
17 investigate the effects of microphysical properties on the evolution of element solubility.

18 2 Methodology

19 2.1 Site description

20 Mt. Lushan is one of the National Geoparks of China, with an area of 302 km², and is situated in
21 northern Jiangxi Province, southern China, adjacent to the Yangtze River and Poyang Lake, which is
22 the largest freshwater lake in China, with an area greater than 4000 km² (Fig. 1). Mt. Lushan is
23 significantly influenced by a subtropical monsoon and mountain climate, with frequent cloud events
24 occurring from spring to autumn. The sampling site is located in Guniubei (115°59'E, 29°35'N, 1165
25 m a.s.l., see Fig. S1), the top of Guling town where most residents work in tourism or related services
26 and little pollution is produced. There are intensive coal-fired power plants located at the eastern
27 coastal area, and abundant mineral resources and many large non-ferrous industries exist in Jiangxi

Comment [It2]: Define the solubility of aerosol elements in this study.

Comment [It3]: Deleted.

Comment [It4]: Add topographical map in the Supplement.

1 and in neighbouring provinces. Therefore, Mt. Lushan is a favourable platform for observing the
2 long-range transport of regional air pollution and for evaluating the influence of atmospheric
3 particles on the local ecological environment.

4 2.2 Sample collection

5 Daily PM_{2.5} samples were collected on quartz fibre filters (MK 360, 90 mm, Munktell, Switzerland)
6 during the summer of 2011 (8 August–23 September) and the spring of 2012 (18 March–20 May).
7 The filters were heated at 500 °C for 3 h prior to sampling, subsequently balanced at 25 °C and 50 ±
8 5% relative humidity for at least 24 h and weighed three times before and after collection. The
9 sampling procedures were conducted during non-rainy and non-cloudy periods by employing a PM_{2.5}
10 impactor (TH-150A, Tianhong Co., China) with a medium flow rate of 100 L min⁻¹. Seventy-six valid
11 ambient samples and 6 blank filters were obtained and stored in the dark and at -20 °C for laboratory
12 analysis.

13 Cloud water were collected by a improved single-stage Caltech Active Strand Cloudwater Collector
14 (CASCC2, see the Supplement for detail). The samples were immediately filtered and stored in
15 brown glass bottles at 4 °C with preservation of 1% v/v high pure hydrochloric acid.

16 The sampling system of cloud residues (Fig. S2) was employed to obtain individual cloud residues
17 in two selected cloud events (on 11 September 2011 and 18 April 2012. Briefly, cloud residues) were
18 trapped onto copper TEM grids coated with carbon film using a single-stage cascade impactor with a
19 0.5 mm-diameter jet nozzle under a flow rate of 0.5 L min⁻¹. An optical microscopy with
20 magnification from ×500 to ×1200 was used to check the integrity of carbon film and particle
21 distribution on the TEM grid. If suitable, the grids were sealed in a dry plastic tube and stored in
22 desiccators at 25 °C and 20 ± 3% RH until the laboratory analysis. Otherwise, another satisfactory
23 sample shall be collected and preserved.

24 More detailed information can be found in (Li et al., 2013).

Comment [It5]: Add the sampling of cloud water in the manuscript and the Supplement.

Comment [It6]: Add the description of sampling system of cloud residues in the manuscript and the Supplement.

Comment [It7]: Add the preparation for individual cloud residues analysis.

1 **2.3 Extraction procedure**

2 **2.3.1 Total fraction (Acid)**

3 To obtain the total concentration of trace elements in fine particles with the least loss of semi-volatile
4 elements, one quarter of the samples and blank filters were digested with an acid mixture (5 mL 65%
5 HNO₃ and 2 mL 30% H₂O₂, guaranteed reagent grade, Kemiou Co., China) in closed Teflon vessels
6 using a microwave digestion system according to a controlled gradient temperature procedure:
7 reaching 120 °C in 5 minutes and remaining there for 5 minutes, then reaching 160 °C in 5 minutes
8 and remaining there for 2 minutes, and finally reaching 185 °C in 5 minutes and remaining there for
9 15 minutes. After cooling to room temperature, the solutions were filtered and subsequently diluted
10 to 25 mL with high-purity deionised water ($\geq 18 \text{ M}\Omega\cdot\text{CM}$) in acid-cleaned brown glass bottles.

11 **2.3.2 Water-soluble fraction (Water)**

12 Half of the samples and blank filters were extracted with 50 mL high-purity deionised water (≥ 18
13 $\text{M}\Omega\cdot\text{CM}$) using ultra-sonication for 1 h followed by filtration. Solutions of approximately 25 mL
14 were preserved in acid-cleaned brown glass bottles with 1% v/v high pure hydrochloric acid to lessen
15 adsorption of the elements by the glass walls. All solutions were stored at 4 °C until instrument
16 analysis.

17 **2.4 Chemical and physical analysis**

18 The concentrations of the total and water-soluble fractions of twelve trace elements (including Al, Cr,
19 Mn, Fe, Cu, Zn, As, Se, Mo, Cd, Ba and Pb) were measured by Inductively Coupled Plasma Mass
20 Spectrometry (ICP-MS, Agilent 7500a) based on the EPA 200.8 method using internal standard
21 substances of Li, Sc, Ge, Y, In, Tb and Bi to eliminate matrix interference. National standard
22 materials (soil, GSS-4, China) were digested for calculating element recoveries by the acid extraction
23 method. All recoveries were found to be a little lower than 100% (Table S1), ranging from 93.0% for
24 Cd to 72.7% for Se, primarily ascribed to volatilisation losses and acid mixture that is not strong
25 enough to release all mineral constituents from the silica matrix into the solution. Reagent and filter

1 blanks were also prepared and analysed for background element content. The detection limits of the
2 ICP-MS analysis for the total fraction elements determined were calculated as three times the
3 standard deviation (3δ) of the six blank values (Table S1 in the Supplement). Trace elements
4 concentrations in cloud water samples were similarly determined by ICP-MS.
5 Individual metal particles in cloud residues on the TEM grids were analysed with a JEM-2100 TEM
6 operating at 200 kV accompanied by a semi-quantitative determination of elemental composition by
7 an energy-dispersive X-ray spectrometer (EDS) that can detect elements heavier than carbon. EDS
8 spectra were collected for only 15 s to minimise radiation exposure and potential beam damage.
9 Copper could not be analysed because of interference from the copper TEM grid.

Comment [It8]: Add the use of ICP-MS to measure trace elements concentrations in cloud water.

10 2.5 Meteorology

11 Meteorology parameters during the observation periods and two cloud events were obtained from the
12 local meteorological station (listed in Table S2). Generally, summer days exhibited higher
13 temperature, relative humidity and wind speed than spring. In particular, the cloud events were
14 characterized by high humidity (>99%), low wind speed (about 1.0 m s^{-1}) and bad visibility (nearly 0
15 km).

Comment [It9]: Add the meteorology information.

16 2.5.2.6 Backward trajectories and potential source contribution function (PSCF)

17 The Hybrid Single-Particle Lagrangian Integrated Trajectory (HYSPLIT) model (PC Version 4.8)
18 developed by the National Oceanic and Atmospheric Administration Air Resources Laboratory
19 (NOAA-ARL) (Draxler and Rolph, 2014) was used to reconstruct the three-dimensional backward
20 trajectories for the purpose of identifying the possible impacts of long-range transport. Three-day air
21 mass backward trajectories initiated every 12 h arriving at Mt. Lushan at the height of 1,165 m a.s.l.
22 were calculated, and five mean trajectory clusters were classified.
23 The potential source contribution function (PSCF) analysis developed by (Hopke et al., 1995) was
24 computed using a geographical information system based software TrajStat (Wang et al., 2009) with
25 the calculated backward trajectories and measured atmospheric pollutant concentrations, representing
26 the conditional probability that air parcels may be responsible for concentrations higher than the

criterion level during transport to the receptor site. The PSCF value for the ij th grid cell is defined as

$$\text{PSCF}_{ij} = \frac{m_{ij}}{n_{ij}} \quad (1)$$

where n_{ij} is the total number of trajectory segment endpoints that fall in the ij th cell and m_{ij} is the number of endpoints for the same cell with arrival times at the sampling site corresponding to pollutant concentrations higher than an arbitrary criterion value. In this study, the total number of endpoints was 18,998, and the geophysical domain (90–130 °E, 15–45 °N) was divided into 4,800 grid cells with a 0.5 ° × 0.5 ° resolution. The average concentrations were set as criteria for PM_{2.5} and each trace element, except for Al, for which the 75th percentile was better to distinguish between larger versus moderate regional sources. The PSCF values were multiplied by an arbitrary weight function W_{ij} to reduce the effect of small values of n_{ij} and to better reflect the uncertainty in values for these cells (Polissar et al., 2001). The weighting function reduced the PSCF values when the total number of the endpoints in a particular cell (n_{ij}) was less than approximately three times the average value (n_{Ave}) of the endpoints per each cell, defined as

$$W_{ij} = \begin{cases} 1.00 & n_{ij} > 3n_{\text{Ave}} \\ 0.70 & 1.5n_{\text{Ave}} < n_{ij} \leq 3n_{\text{Ave}} \\ 0.42 & n_{\text{Ave}} < n_{ij} \leq 1.5n_{\text{Ave}} \\ 0.17 & 0 < n_{ij} \leq n_{\text{Ave}} \end{cases} \quad (2)$$

3 Results and discussion

3.1 Elemental composition

3.1.1 General characterisation

The ambient atmospheric concentrations of PM_{2.5} and trace elements including total and water-soluble fractions at Mt. Lushan are summarised in Table 1, and the comparison with typical mountains and megacities in China are listed in Table S3[†]. The average PM_{2.5} concentration at Mt. Lushan in spring (54.7 µg m⁻³) was approximately that of summer (55.9 µg m⁻³), more than twice the WHO air quality guideline for daily PM_{2.5} of 25 µg m⁻³, but still lower than many urban sites at ground level such as Beijing (118.5 µg m⁻³) and Guangzhou (81.7 µg m⁻³) (Yang et al., 2011). It was

1 clearly contrary to Mt. Tai (Deng et al., 2011), where PM_{2.5} exhibited a concentration 2–3 times
2 higher in summer (123.1 µg m⁻³) than in spring (46.6 µg m⁻³), suggesting a less-pronounced seasonal
3 variation of PM_{2.5} at Mt. Lushan.

4 The total fraction concentrations of twelve trace elements in spring were comparable with those in
5 summer at Mt. Lushan, with the exception of higher Al in spring. Overall, elements Al and Fe
6 contributed to the highest concentration, and the other elements decreased from 258.3 ng m⁻³ for Zn
7 to 2.0 ng m⁻³ for Mo. The dominant elements (Al, Fe and Zn) exhibited significantly lower
8 concentrations at Mt. Lushan than Mt. Tai (1200 ng m⁻³ for Al, 810 ng m⁻³ for Fe and 400 ng m⁻³ for
9 Zn) (Deng et al., 2011) and slightly higher than Mt. Gongga (295.8 ng m⁻³ for Al, 224.0 ng m⁻³ for Fe
10 and 154.6 ng m⁻³ for Zn) (Yang et al., 2009a), probably due to the geomorphology and climatology
11 biases. As shown in Table S34, all elements (except Ba) have lower concentration levels in
12 comparison with Mt. Dinghu, a national nature reserve influenced by atmospheric pollution (Yang et
13 al., 2009b) and with typical megacities in China such as Beijing, Guangzhou (Yang et al., 2011) and
14 Shanghai (Chen et al., 2008). For water-soluble fractions, Zn transformed into the primary elements,
15 followed by Al and Fe, with higher concentrations in summer than spring; other trace elements (from
16 Pb to Mo) were still comparable between summer and spring.

Comment [lt10]: Corrected.

17 3.1.2 Temporal variations

18 Figure 2 displays the temporal variations of trace element concentrations in PM_{2.5} at Mt. Lushan for
19 total and water-soluble fractions during the sampling campaigns. Most total fraction elements
20 exhibited more intense variances in spring than in summer, with unique temporal patterns such as the
21 highly variable pattern observed for aluminium and the relatively steady pattern of arsonium. Similar
22 temporal patterns were observed for the water-soluble and total fractions for most elements, except
23 for Al and Fe, which had drastic variations with many spike episodes for total fractions but lower
24 constant concentration for water-soluble fractions. The dependence of temporal variations of
25 water-soluble elements on their total fractions were also examined (Fig. S34). The concentrations of
26 water-soluble Zn, Cu, Mn, As, Se and Cd were found to be rather consistent with their total fraction
27 according to their high correlations ($R^2 = 0.50\text{--}0.78$), whereas there was only a weak association

1 between the total concentrations and water-soluble fractions of Al, Fe and Cr.
2 Several spikes in element concentration were observed in specific periods. The first spike (Spike I)
3 for all elements from 11–13 August 2011 was ascribed to the short sampling time due to the
4 interruption by an unexpected thundershower. However, the significantly elevated total concentration
5 of Al, Fe and Mn during 23–25 March 2012 (Spike II) and 25–26 April 2012 (Spike III) with no
6 distinct elevation in the other elements were observed (Fig. 2), likely contributed by the dust storms
7 originating from the Gobi desert and the Taklimakan desert in spring according to the MODIS image,
8 the OMI Aerosol Index and air mass backward trajectory analysis (Fig. S42). These features were
9 similar with the Asian Dust observed at Huaniao Island in the East China Sea, where concentrations
10 of Al, Fe, Mn and Ba 3–4 times higher were observed with no significant difference for Zn, Cu, As
11 and Cd in the air compared with non-dust days (Guo et al., 2014b). In addition, the dust storms
12 contributed little to the water-soluble fractions of all trace elements.

13 3.2 Source identification

14 3.2.1 Correlations between individual elements

15 The Pearson correlation coefficients r between each element for both total fraction and water-soluble
16 fraction were examined (Table S43). Moderate significant associations of Fe with elements Al, Mn
17 and Cr are found to exist both in total and water-soluble fractions with comparable coefficients
18 between 0.40–0.68. Correlations for other trace elements in water-soluble fraction are stronger than
19 in total fraction, suggesting the higher possibilities of common sources for some water-soluble
20 elements. For example, the correlation levels of Zn–Cu, Zn–Se, Pb–Zn and Pb–Se are dramatically
21 high for water-soluble fractions ($0.72 < r < 0.82$) and moderate for total fractions ($0.25 < r < 0.52$),
22 which could be attributed to their common anthropogenic sources of coal-fired power plants and
23 industrial processes based on the suggestion of the spherical morphology and elemental composition
24 of individual metal particles via the TEM examination (Li et al., 2014).

25 3.2.2 Anthropogenic pollution

26 The enrichment factor (EF) for individual trace elements was applied to identification of their

Comment [lt11]: Corrected.

1 general crustal and anthropogenic sources and evaluate the degree of pollution using the following
2 formula:

$$3 \quad EF_i = (X_i / X_R)_{\text{aerosol}} / (X_i' / X_R')_{\text{crust}} \quad (2)$$

4 where EF_i is the enrichment factor of element i ; X_i and X_R are the concentrations of element i and
5 reference element R in aerosol, respectively; X_i' and X_R' are the background contents of elements in
6 Chinese soils (Wei et al., 1991); and Al is selected as the reference element for calculation. Element
7 sources are classified into three groups with the following standard: $EF < 10$ is considered to be a
8 crustal origin without enrichment; $10 < EF < 100$ comes from mixed origins (crustal and
9 anthropogenic sources); $EF > 100$ indicates air pollution from an anthropogenic origin. Figure 3
10 describes the EF values for both the total and water-soluble fractions of each element in a decreasing
11 order. Elements with $EF > 100$, including Se, Cd, Zn, Pb, As, Mo and Cu, were found to be highly
12 enriched, ranging from hundreds to tens of thousands in both fractions, indicating the severe
13 anthropogenic pollution of atmospheric trace elements. Cr, Ba and Mn were likely to be from mixed
14 origins because the majority of their EF values fell within 10–100. Fe was predominantly from a
15 crustal origin based on its $EF < 10$. It is worth noting that the water-soluble fractions of most
16 elements (except Cr and Fe) have higher EF values by approximately one order of magnitude than
17 the total fractions, especially for elements with extremely high EF values, implying the inclination of
18 enormous pollution toward the water-soluble fraction of anthropogenic elements.

19 **3.2.3 Emission source classification**

20 The principal component analysis (PCA) was performed in detail to classify the main sources of
21 trace elements in $PM_{2.5}$ at Mt. Lushan. The PCA results for trace elements in total fraction are shown
22 in Fig. 4 with four major components identified.

23 The first principal component was considered primarily from nonferrous metal mining and
24 metallurgical smelting, accounting for 34.4% of the total variance with high loadings for Cr, As, and
25 Ba and considerable loadings for Zn and Mo. Although there were diverse EF values which
26 suggested anthropogenic origins mixed with crustal materials ranging from dozens for Cr and Ba to
27 thousands for As, Zn and Mo, these total fraction elements still presented considerably moderate

1 correlations. According to the provincial output statistics of nonferrous metals in 2010 (Cheng et al.,
2 2015) and the Overall Planning of Mining Resources of 2008–2015 for Jiangxi and adjacent Hunan
3 Province, there are abundant nonferrous minerals (such as barite, realgar and sphalerite, etc.) and
4 many large-scale metallurgical industries within and near Jiangxi Province. In addition, high
5 concentrations of Pb and Zn in cloud drop residues at Mt. Lushan were suggested deriving from fine
6 particles contributed by nonferrous smelting in Jiangxi Province (Li et al., 2013).

7 The second principal component that contributed to high loadings for Pb, Cu, Se, Zn, and Mn was
8 identified as coal combustion. Coal combustion is representatively considered to be the source of
9 most atmospheric trace elements in China. All species in this component except Mn exhibited high
10 EF values, indicating their anthropogenic origins. The semi-volatile Se is usually used as a tracer for
11 determining atmospheric sources and even the pathways of coal combustion pollutants, because it is
12 primarily produced in high temperature combustion and can undergo long-range transport with fine
13 particles after the rapid gas-to-particle conversion (Husain et al., 2004; Wen and Carignan, 2007).

14 Coal combustion is also becoming the major contributor to atmospheric Pb with the nationwide
15 phase-out of leaded gasoline in China (Xu et al., 2012). The high correlations between Se and the
16 other species in Component 2 clearly indicated the likely sources of coal combustion.

17 The third component in particular explained most of the Al and Fe which are the typical signatures of
18 crustal materials or soils, along with relatively high correlations and low EF values.

19 Municipal solid waste incineration was regarded as the primary sources of fine particle Cd and Mo at
20 Mt. Lushan, explaining 8.4% of the variance. Both Cd and Mo had low concentrations but high EF
21 values, with a strong association in total fraction ($r = 0.71$). Jakob et al., (1995) found that Cd in fly
22 ash of municipal solid waste incinerators could evaporate into the atmosphere completely during heat
23 treatment. The rapid increase in atmospheric Cd emissions from municipal solid waste incineration
24 in recent years and the unbalanced large emissions in east-central and southeast China (Tian et al.,
25 2012) were responsible for fine particle Cd at Mt. Lushan.

26 **3.3 Potential source region distributions**

27 Three-day air mass backward trajectories were calculated to estimate the potential source regions and

1 pathways of air pollutants, making full use of the geographical advantages of the high-altitude
 2 observation site and the long-range transport capacity of fine particles. The air masses associated
 3 with PM_{2.5} samples were classified into five clusters (Fig. 5a). The air masses of the Southwest (SW)
 4 cluster originated from the South China Sea and passed through the Pearl River Delta (PRD), Hunan
 5 and Jiangxi Province with the highest occurrence frequency of 28.9%. Cluster East (E) mainly came
 6 from the East China Sea and partly from the Circum-Bohai Sea Region, traversing the Yangtze River
 7 Delta (YRD) and Anhui Province at a frequency of 27.6%. Air masses of cluster Local (L) were
 8 found to be advancing toward or revolving around Mt. Lushan slowly from ground-level within areas
 9 covering distances of approximately 200 km away from the observation site, contributing 22.4% of
 10 the occurrence frequency. Clusters Northwest (NW) and North (N) both went through the China
 11 Loess Plateau and accounted for 13.2 and 7.9% of the occurrence frequency, respectively. The
 12 primary difference was that the former mainly originated from Taklimakan and the Gobi Desert,
 13 whereas the latter was from remote Siberia and Mongolia with a much higher wind speed.

14 Figure 5b shows the averaged PM_{2.5} concentration of different clusters. Cluster E exhibited the
 15 highest PM_{2.5} concentration of 67.0 $\mu\text{g m}^{-3}$, followed by cluster L (59.6 $\mu\text{g m}^{-3}$) and the similar
 16 clusters NW and N, whereas cluster SW had the lowest concentration (45.3 $\mu\text{g m}^{-3}$). The order of
 17 PM_{2.5} concentration seemed to be consistent with the PSCF result (Fig. 5c) which integrated PM_{2.5}
 18 concentration with air mass occurrence frequency. As shown in Fig. 5c, the YRD and southern Anhui
 19 Province were the most likely source regions of PM_{2.5} at Mt. Lushan. These economically developed
 20 regions exhibit massive energy consumption and industrial production, becoming important
 21 anthropogenic source regions in eastern China. The local area of Jiangxi, neighbouring southern
 22 Anhui and eastern Hunan were also significant PM_{2.5} source regions, where many nonferrous metal
 23 smelting industries are widely distributed. However, the contributions to PM_{2.5} at Mt. Lushan by
 24 long-range transport of air masses from northern China (Inner Mongolia and the Loess Plateau) were
 25 much less than from eastern China and local regions, suggesting nearly negligible impacts of mineral
 26 dusts or soil transport on fine particle mass concentration at Mt. Lushan compared with regional
 27 anthropogenic pollution. In addition, the PM_{2.5} concentration in five clusters or different source
 28 regions were highly dependent on the inorganic ions, especially the secondary ions (Li et al., 2014).

1 Interestingly, the PRD contributed much less concentrations to fine particles in spite of its high
2 occurrence frequency, probably due to particle scavenging by frequent rainfall during the Asian
3 summer monsoon.

4 Figure 6a–l illustrates the distinctive potential source region distributions for individual elements in
5 fine particles at Mt. Lushan. Crustal elements Al and Fe exhibited similar source region distributions
6 (Fig. 6a and b). The highest PSCF values in northern China including the Loess Plateau, Henan and
7 eastern Hubei Province indicated that these areas were very important source regions and pathways
8 for fine particle Al and Fe, with vast contributions of long-range transport of mineral dusts or soils.
9 The PRD and eastern Hunan Province were likely to be other important source regions for Al and Fe
10 probably due to the influence of mining activities, whereas the YRD in eastern China and the local
11 area of Jiangxi Province made much lower contributions.

12 Fine particle As (Fig. 6c) had an almost parallel pattern of source region distribution with Fe, except
13 the discordance that the PRD, eastern Guangxi, Hunan and Jiangxi Province were identified as the
14 most important source regions and pathways, attributable to the emissions of the nonferrous metals
15 mining and smelting industries. Northern China also tended to be an important potential source
16 region, suggesting the possible contribution of natural sources for As. Similar to As, the PRD, Hunan
17 and Jiangxi Province, as well as northern China were also potential source regions for fine particle
18 Mn (Fig. 6d). However, the YRD area was characterised by extremely high PSCF values for Mn,
19 indicating an important anthropogenic source region.

20 Fine particle Pb, Zn, Cu and Se (Fig. 6e–h), which were identified primarily from coal combustion
21 by the PCA analysis, had similar source region distributions with some discrepancies, generally
22 coinciding with the geographical distribution of coal-fired power plants in China which were
23 aggregated within coastal areas such as the YRD, the PRD and Shandong Province (Fig. S53a). The
24 YRD area including Jiangsu, Zhejiang and southern Anhui Province was an especially pronounced
25 source region for Pb, Zn, Cu and Se at Mt. Lushan. The significantly high PSCF values in the YRD
26 region were attributable to the large coal consumption by intensive power plants in Jiangsu, Zhejiang
27 and even Shandong Province and to the differences in trace element contents in raw coal such as high
28 Se contents in Anhui Province, both of which made great contributions to emissions of atmospheric

1 trace elements (Tian et al., 2014). Meanwhile, the PRD, Hunan and the local area of Jiangxi Province
2 also played a remarkable role in source region distributions of Zn, Cu and Se at Mt. Lushan, for
3 which coal-fired power plants and nonferrous metals smelting industries in these areas were
4 primarily responsible. Unexpectedly, northern China rather than the PRD area was also identified as
5 a potential source region of Pb, possibly attributed to the partial contributions of long-range transport
6 of mineral dusts for fine particle Pb at Mt. Lushan.

7 As shown in Fig. 6i and j, the YRD, the PRD, eastern Hunan and western Jiangxi were identified as
8 the common likely source regions and pathways for fine particle Cd and Mo at Mt. Lushan. The
9 identified source regions corresponded very well with the uneven regional distribution of municipal
10 solid waste (MSW) incineration plants in China (Fig. S53b), with 183.5, 175.1 and 146.6 kg of
11 atmospheric Cd emitted by MSW incineration from Jiangsu, Zhejiang and Guangdong, respectively,
12 the top three largest emitting provinces in 2010 (Tian et al., 2012). Figure 6k shows an apparently
13 more homogeneous source region distribution for Ba, with the PRD and areas surrounding Mt.
14 Lushan as potential source regions which have a high natural background content of barite. On the
15 contrary, few potential source regions were identified for Cr (Fig. 6l) besides the PRD, parts of
16 Hunan Province and a small region in central Zhejiang with low PSCF values.

17 It should be noted that the potential source region distributions for trace elements at Mt. Lushan were
18 very different with PM_{2.5}. The YRD, the PRD and Hunan Province were likely to be the major source
19 regions for most anthropogenic elements (except Cu within eastern Jiangxi), and northern China was
20 likely for crustal elements (Al and Fe). However, the contribution probabilities of areas near Mt.
21 Lushan for most elements were obviously lower than other source regions. ~~That~~ This result revealed
22 that long-range transport and regional anthropogenic sources, rather than local sources, made much
23 more significant contributions to fine particle trace elements at Mt. Lushan, which could be ascribed
24 to the different types and quantities of emissions as well as the protection policies for Mt. Lushan
25 and its adjacent Poyang Lake.

26 In addition, the order of mass concentration of individual trace elements for five air mass clusters
27 ending at Mt. Lushan (Fig. S64) was in accordance with the distributions of likely source regions
28 identified by PSCF values, further suggesting greater contributions by regional sources and

Comment [It12]: Corrected.

1 long-range transport to fine particle trace elements at Mt. Lushan. For example, clusters N and NW
2 contributed ~~to~~ the highest concentration for crustal Al and Fe and anthropogenic Zn and As, followed
3 by the highest cluster SW, E and the lowest cluster L; exceptionally, cluster L made the highest
4 contribution to the combustion element Cu.

Comment [It13]: Corrected.

5 3.4 Trace element solubility

6 3.4.1 Comparison of individual element solubility

7 In this study, element solubility is calculated ~~defined~~ as the percentage of water-soluble
8 concentrations of an element divided by its total concentration. Figure S75 compares the average
9 water solubility of individual elements in PM_{2.5} at Mt. Lushan with other sites in decreasing order.
10 The most soluble elements were As, Mn, Cu, Zn and Se with a solubility reaching up to 60–70%;
11 followed by Cd, Pb, Ba and Mo with moderate solubility, approximately 40–50%; whereas the least
12 soluble elements were Fe, Al and Cr with a solubility less than 30%. Compared with TSP over the
13 East China Sea (Hsu et al., 2010), some elements (Mn, Cu, Ba, Mo, Fe and Al) were significantly
14 highly soluble in PM_{2.5} at Mt. Lushan, whereas other species (As, Zn, Se and Cd) showed the
15 opposite with the exception of comparable Pb and Cr. Similarly, compared with the PM_{2.5} at
16 Edinburgh, UK (Heal et al., 2005), the elements Mn, Cu and Fe exhibited higher water solubility,
17 whereas the elements As, Zn and Pb were comparable, and the elements Cd and Cr were lower at Mt.
18 Lushan. A large gap in anthropogenic elements (As, Mn, Cu and Pb) between Mt. Lushan and
19 Nanjing (Hu et al., 2012) was also observed. Experimental conditions (compared in Supplement
20 Table S5) such as digestion methods or analysis instruments may result in ~~the some~~ solubility
21 discrepancies at different sites, but they are far from the determinant.

Comment [It14]: Add the detailed comparison of various experimental conditions.

22 3.4.2 Effect of emission sources on element solubility

23 Element solubility is associated with four major emission sources identified by EF value and PCA
24 analysis and displayed in Fig. 7. Crustal elements with mean EF < 10 had low average solubility (<
25 30%) besides the highly dissolved Mn that was possibly impacted by a combustion source; the
26 solubility of elements related to mining and metallurgy varied between < 10%–70% with a 10–1000

1 range in EF value; coal combustion elements characterised by high EF values over 100 exhibited a
2 high solubility of approximately 45%–75%, contributable to the combustion process during which
3 oxidisable elements in coal are mostly altered to easily soluble species (Quispe et al., 2012);
4 elements produced by waste incineration were also highly soluble (40%–50%) coupled with EF >
5 100. The roughly increasing tendency of solubility along with EF value suggested that element
6 solubility was closely related to the emission sources, likely indicating that crustal elements with low
7 EF values often showed low solubility, whereas polluted elements featuring high EF values were
8 usually highly soluble. This result coincides well with the conclusion that the dissolvable portion of
9 aerosol elements is controlled by their dominant crustal or anthropogenic origins (Hsu et al., 2005).
10 However, there are also some exceptions that could not be explained by emission sources. For
11 instance, the low solubility of atmospheric Cr at Mt. Lushan could probably be ascribed to the stable
12 crystalline structure in minerals such as chromite, with the reduced Cr (III) being the dominant
13 species in ambient fine particles (Werner et al., 2007). Figure S86 further shows a hyperbolic or
14 negative logarithmic relationship between element concentration and the solubility for and only for
15 Al, Fe, Cr and Mn, similar to many inverse relationships for aerosol Fe, Al and other species
16 reviewed by (Schulz et al., 2012), indicating the unneglected effect of total concentration on crustal
17 trace element solubility rather than anthropogenic elements. Thus, trace element solubility may be
18 initially determined by emission sources with various interference.

19 3.4.3 Source region contributions to element solubility

20 Figure 8 illustrates the potential source regions for individual element solubility in PM_{2.5} at Mt.
21 Lushan with the expanding application of PSCF analysis to evaluate the local and regional
22 contributions. It can be seen that almost all of the elements had quite different solubility distributions
23 with their total concentrations, characterised by the highest PSCF values for element solubility in the
24 local area of Jiangxi Province and the YRD region followed by lower PSCF values in parts of the
25 PRD region and Hunan Province.

26 In this study, we used fine particle Fe for detailed explanation because there are many investigations
27 on the solubility of aerosol Fe, which plays a critical role in the global iron cycle among terrestrial

1 dust, the atmosphere and the ocean, as well as in the effects on climate (Jickells et al., 2005). As
 2 shown in Fig. 8a, northern China, identified as the major source region for crustal Fe, made little
 3 contribution to its solubility. The significantly low solubility of fine particle Fe in northern China,
 4 much lower than the PSCF criteria value, was consistent with the very low soluble Fe (solubility less
 5 than 2%) from desert dusts or soils (Baker et al., 2006; Jickells et al., 2005). The experiment
 6 performed by (Mackie et al., 2006) suggests that the amount of readily released Fe does not increase
 7 after the uplift and abrasion of soils in areas with little atmospheric pollution; thus, the low solubility
 8 of the Fe from northern China could be attributed to the initial absence of dissolved Fe in dusts or
 9 soils derived from the Gobi desert or Loess Plateau. On the contrary, the relatively much higher
 10 PSCF values for Fe in the local area of Jiangxi, southern Anhui and the YRD indicated greater
 11 contributions of anthropogenic pollution in these regions to the solubility of fine particle Fe at Mt.
 12 Lushan, because the high solubility of Fe in the YRD and Anhui Province was just in accordance
 13 with the large amounts of anthropogenic emissions of SO₂ and NO_x in these regions (Zhang et al.,
 14 2009), which could significantly promote the dissolution of aerosol Fe acting as acid precursors
 15 (Schulz et al., 2012; Solomon et al., 2009). A significant correlation (0.629) of iron solubility and
 16 sulphate concentration in our fine particle samples was further verified, similar to the correspondence
 17 of high iron solubility to the sulphur content in ambient fine particles observed by (Oakes et al.,
 18 2012). Moreover, the outstanding enhancement of fine particle Fe solubility in local regions close to
 19 Mt. Lushan was principally recognised to be an effect of cloud processing, an important atmospheric
 20 process controlling Fe dissolution in aerosols (discussed in Sect. 3.4.4). The regional distributions for
 21 the solubility of crustal Al was similar with Fe, except for the lower PSCF values near Mt. Lushan
 22 (Fig. 8b).
 23 Anhui, Jiangsu and Jiangxi Province were identified as the most important contributors to the high
 24 solubility of fine particle As at Mt. Lushan (Fig. 8c), ascribed to the large amount of atmospheric As
 25 emissions from anthropogenic sources (approximately 200 tons in 2010) in these provinces (Cheng
 26 et al., 2015); in contrast, little contributions were made to As solubility by the PRD and Hunan
 27 Province where the highest As concentrations were provided. For the elements from coal combustion
 28 (including Mn, Pb, Zn, Cu and Se, Fig. 8d–h) and MSW incineration (including Cd and Mo, Fig. 8i

1 and j), the highest contributions of element solubility were uniformly focused within the local area of
2 Jiangxi Province, the YRD and parts of Fujian Province, generally coinciding with their significantly
3 high concentrations emitted from anthropogenic sources in eastern China. The solubility pattern for
4 Ba (Fig. 8k) was rather similar to its concentration distribution, whereas the pattern of high solubility
5 for Cr in Anhui Province (Fig. 8l) was very different to the concentration pattern.

6 It can be concluded that the solubility of fine particle trace elements from local and regional source
7 regions were much higher than that by long-range transport from south-western China and northern
8 China. The high contributions for particle element solubility in the YRD region should be attributed
9 to the serious air pollution. However, on account of the relatively less air pollution released from
10 local sources, the frequent cloud processing was considered as the significant contributor to the high
11 solubility of trace elements in local regions near Mt. Lushan.

12 Additionally, the statistics on the solubility of individual fine particle elements at Mt. Lushan for five
13 air mass categories are shown in Fig. S97. In general, the fine particle elements derived from cluster
14 L exhibited the highest solubility whether for crustal or anthropogenic elements, closely followed by
15 cluster E; elements from cluster SW showed moderate solubility, ascribed to the wash-out of soluble
16 constituents by frequent rainfall in summer monsoon; elements from cluster NW and N were the
17 least soluble, primarily impacted by crustal materials from northern China. It was demonstrated that
18 the statistical results for most elements fairly agreed with the solubility distributions identified by
19 PSCF analysis.

20 **3.4.4 Evolution of element solubility during cloud processing**

21 Cloud processing might be of great importance in affecting aerosol dissolution at Mt. Lushan where
22 frequent cloud events occurred. To determine the evolution of element solubility during cloud
23 processing with less disturbance of natural factors and human activities, cloud events were selected
24 with the following conditions: (1) non-raining cloud to avoid scavenging of particles by precipitation,
25 (2) short duration and time interval of cloud processing and particle sampling to minimise the
26 interference of external aerosols, (3) identical air mass trajectory of the cloud and particles with low
27 wind speed to ensure consistent origins of the air masses. Table S64 shows the alteration of

individual element solubility in fine particles before and after the two selected cloud events on 11 September 2011 and on 18 April 2012.

It was evident that after cloud processing on 11 September 2011, most fine particle elements exhibited a drastic increase in solubility. For instance, post-cloud particle Al became much more soluble compared with the pre-cloud particle, with solubility changing from 1.7 to 28.7%. Other elements, such as Cu, Zn, As, Se, Cd and Ba, also showed an approximately one- to two-fold increase in solubility. The cloud processing on 18 April 2012 also brought about a significantly large number of solubility increments for the crustal elements Al and Fe, but it resulted in less increments for anthropogenic elements such as Cu, As, Se and Pb due to their already higher solubility in pre-cloud particles which might have undergone intensive cloud cycles during the prolonged residence time in the air. Generally, the evidently higher solubility for the post-cloud fine particle elements after the two cloud events, overpassing their overall average solubility, corroborated the remarkable dissolution efficiencies of aerosol elements by cloud processing at Mt. Lushan.

Interestingly, the increase in aerosol element solubility after both cloud events was coupled with the elevation of aerosol sulphate concentration as shown in Table S64. For example, post-cloud sulphate particles (4 h) exhibited a sharp elevation of $10 \mu\text{g m}^{-3}$ after the cloud processing (3 h) on 11 September 2011. Based on the very short intervals between cloud events and post-cloud particle sampling, the increased sulphate particles were most likely contributed by cloud water sulphate, which could be generated by the rapid atmospheric aqueous-phase oxidation of S(IV) with a rate greater than $100\% \text{ h}^{-1}$ (Seinfeld and Pandis, 2012), much quicker than the gas-phase oxidation of SO_2 with a rate of approximately $1\% \text{ h}^{-1}$ (Newman, 1981). In addition, the higher sulphate concentrations in cloud water and post-cloud particles on 11 September 2011 (41.70 mg L^{-1} and $24.72 \mu\text{g m}^{-3}$, respectively) from cluster E compared with those on 18 April 2012 (26.78 mg L^{-1} and $17.34 \mu\text{g m}^{-3}$, respectively) from cluster L were likely to be associated with the larger amount of anthropogenic SO_2 gases from the YRD in eastern China because acidic substances, such as sulphate formed by their precursor gases (e.g., SO_2), are prone to exist in fine particles and lead to acidification of aerosols (Ren et al., 2011); and the pH of cloud droplets modified by these dissolved acidic substances in particles could in turn influence the dissolution of aerosol trace elements (Deguillaume

1 et al., 2005). As a consequence, the enhancement of trace element solubility during cloud processing
2 were probably dependent on the corresponding heterogeneous formation of sulphate.

3 To further understand the effect of cloud processing on aerosol elements dissolution, individual cloud
4 droplet residues were collected during the two cloud events, and the micro-morphology and
5 composition of metal particles were examined by TEM-EDS analysis. Representative TEM images
6 and the EDS spectra of major metal particles are shown in Fig. 9. Plenty of Pb-rich, Fe-rich and fly
7 ash particles were observed to be the dominating metal particles in the two cloud events, consistent
8 with the major types of metal-associated particles (Pb-rich, fly ash, Fe-rich and Zn-rich) in cloud
9 droplets at Mt. Lushan (Li et al., 2013). Almost all of metal particles were found to be internally
10 mixed within S-rich cloud residues with the encapsulation of cloud water and presented a nearly
11 spherical shape or aggregation, suggesting the likely sources to be high-temperature coal combustion
12 by coal-fired power plants and industries, during which industrial gases containing abundant SO₂ and
13 metals were released, followed by the generation of metal-sulphate particles (Gieré et al., 2006).

14 Figure 9 also demonstrates the small diameters of the metal particles in cloud residues much smaller
15 than 1 µm, especially for the aggregation of spherical Fe nanoparticles embedded in aged S-rich
16 residues (Fig. 9c). The unique, large specific surface of nano-sized Fe particles is able to effect a
17 higher absorption intensity and more complicated surface chemistry during cloud processing,
18 generating greater quantities of surface complexes with acidic anions such as sulphate, and
19 improving the dissolution rates of iron particles (Rubasinghege et al., 2010). Shi et al. (2009)
20 suggested that the variations in pH during cloud processing would induce the formation of
21 amorphous Fe nanoparticles and an increase in iron solubility (reactivity) in Saharan dusts. More
22 importantly, the solubilisation of aerosol elements caused by the change in particle morphology
23 during cloud processing is irreversible (Deguillaume et al., 2005). Finally, along with the dissipating
24 of cloud water in droplets, the Fe nanoparticles and sulphate residues remain in post-cloud particles,
25 resulting in an attractive enhancement of Fe solubility. Therefore, we hypothesise that irreversible
26 changes or alterations of particle morphology such as specific surface area, which may result from
27 the acidification and heterogeneous reactions during cloud processing, should be the critical factor
28 for the significant enhancement of solubility not only for Fe, but also for many other trace elements

1 in cloud-processed fine particles.

2 **4 Conclusions**

3 The characteristics of fine particle trace elements at the summit of a mountain in southern China
4 were investigated. The PM_{2.5} concentration ($55.2 \pm 20.1 \mu\text{g m}^{-3}$) was twice the WHO guideline but
5 much lower than that in urban sites, with little seasonal variation. The total fractions of Al and Fe and
6 the water-soluble fraction of Zn were the dominant elements and similar temporal variations between
7 the total and water-soluble fractions for all species along with several spikes contributed by dust
8 storms for Al and Fe were observed. The enrichment factor analysis implied the pollution trace
9 elements to be more easily concentrated in water-soluble fractions with higher correlations.
10 Nonferrous metal mining and smelting, coal combustion, crustal materials and municipal solid waste
11 incineration were further classified as the major emission sources, which might initially determine
12 the trace element solubility with interferences such as total concentrations. The YRD including
13 Jiangsu, Zhejiang and parts of Anhui Province were indicated as the most important source regions
14 of PM_{2.5} by trajectory cluster analysis and PSCF results, and this result was discrepant with the
15 source distributions for individual trace elements. The YRD as well as the PRD, eastern Hunan and
16 western Jiangxi were identified as the primary source regions and pathways for combustion-related
17 elements (Mn, Pb, Zn, Cu, Se, Cd and Mo) emitted by regional coal-fired power plants and
18 municipal solid waste incineration, whereas the long-range transport of mineral dusts from northern
19 China was the major contributor to crustal Al and Fe. Interestingly, local sources contributed
20 relatively less to most trace elements. In contrast, the YRD region and the local area of Jiangxi
21 Province were very likely to make the greatest contributions to element solubility rather than
22 long-range transport from northern or southern China. A significant enhancement in trace element
23 solubility and corresponding increase in aerosol sulphate were observed during two selected cloud
24 events. TEM-EDS analysis of cloud residues suggested that the irreversible alteration of particle
25 morphology by heterogeneous reactions or acidification with sulphate during cloud processing could
26 crucially increase element solubility.
27 This study highlighted the contributions of regional anthropogenic pollution and local cloud
28 processing to trace element solubility of PM_{2.5} at Mt. Lushan. We further expect that fine particles

1 | ~~w~~eould undergo several cloud-processing cycles during long-range transport with massive clouds
2 | covering the surface of the earth, ~~which can promoteing trace-aerosol elements~~ dissolution and
3 | increas~~e~~~~ing~~ health and ecological risks.

Comment [lt15]: Modified.

4 | **Acknowledgements**

5 | This research was funded by the National Natural Science Foundation of China (21177073 and
6 | 41075092). We acknowledge the NOAA Air Resources Laboraroty (ARL) for provision of the
7 | HYSPLIT trajectory model. We are grateful for all the staff of Lushan Mountain Meteorological
8 | Station for offering the observation platform and their assistance during the field campaigns. Thanks
9 | also due to Taixing Yue at Environmental Monitoring Central Station of Shandong Province for the
10 | help in the ICP-MS measurements.

11

1 **References**

- 2 Baker, A. R., Jickells, T. D., Witt, M., and Linge, K. L.: Trends in the solubility of iron, aluminium,
3 manganese and phosphorus in aerosol collected over the Atlantic Ocean, *March Chem.*, 98, 43-58,
4 doi:10.1016/j.marchem.2005.06.004, 2006.
- 5 Cakmak, S., Dales, R., Kauri, L. M., Mahmud, M., Van Ryswyk, K., Vanos, J., Liu, L.,
6 Kumarathanan, P., Thomson, E., Vincent, R., and Weichenthal, S.: Metal composition of fine
7 particulate air pollution and acute changes in cardiorespiratory physiology, *Environ. Pollut.*, 189,
8 208-214, doi:10.1016/j.envpol.2014.03.004, 2014.
- 9 Cao, J., Xu, H., Xu, Q., Chen, B., and Kan, H.: Fine particulate matter constituents and
10 cardiopulmonary mortality in a heavily polluted Chinese city, *Environ. Health Perspect.*, 120,
11 373-378, doi:10.1289/ehp.1103671, 2012.
- 12 Charrier, J. G., McFall, A. S., Richards-Henderson, N. K., and Anastasio, C.: Hydrogen peroxide
13 formation in a surrogate lung fluid by transition metals and quinones present in particulate matter,
14 *Environ. Sci. Technol.*, 48, 7010-7017, doi:10.1021/es501011w, 2014.
- 15 Chen, J., Tan, M., Li, Y., Zheng, J., Zhang, Y., Shan, Z., Zhang, G., and Li, Y.: Characteristics of
16 trace elements and lead isotope ratios in PM(2.5) from four sites in Shanghai, *J. Hazard. Mater.*, 156,
17 36-43, doi:10.1016/j.jhazmat.2007.11.122, 2008.
- 18 Chen, Y., Ebenstein, A., Greenstone, M., and Li, H.: Evidence on the impact of sustained exposure to
19 air pollution on life expectancy from China's Huai River policy, *Proc. Natl. Acad. Sci. U.S.A.*, 110,
20 12936-12941, 2013.
- 21 Cheng, K., Wang, Y., Tian, H., Gao, X., Zhang, Y., Wu, X., Zhu, C., and Gao, J.: Atmospheric
22 Emission Characteristics and Control Policies of Five Precedent-Controlled Toxic Heavy Metals
23 from Anthropogenic Sources in China, *Environ. Sci. Technol.*, 49, 1206-1214,
24 doi:10.1021/es5037332, 2015.
- 25 Cheung, K., Shafer, M. M., Schauer, J. J., and Sioutas, C.: Diurnal trends in oxidative potential of
26 coarse particulate matter in the Los Angeles Basin and their relation to sources and chemical
27 composition, *Environ. Sci. Technol.*, 46, 3779-3787, doi:10.1021/es204211v, 2012.
- 28 Clements, A. L., Buzcu-Guven, B., Fraser, M. P., Kulkarni, P., and Chellam, S.: Role of particulate

1 metals in heterogenous secondary sulfate formation, *Atmos. Environ.*, 75, 233-240,
2 doi:10.1016/j.atmosenv.2013.04.038, 2013.

3 Costa, D. L., and Dreher, K. L.: Bioavailable transition metals in particulate matter mediate
4 cardiopulmonary injury in healthy and compromised animal models, *Environ. Health Perspect.*, 105,
5 1053-1060, 1997.

6 Deguillaume, L., Leriche, M., Monod, A., and Chaumerliac, N.: The role of transition metal ions on
7 HO x radicals in clouds: a numerical evaluation of its impact on multiphase chemistry, *Atmos. Chem.*
8 *Phys.*, 4, 95-110, 2004.

9 Deguillaume, L., Leriche, M., Desboeufs, K., Mailhot, G., George, C., and Chaumerliac†, N.:
10 Transition metals in atmospheric liquid phases: Sources, reactivity, and sensitive parameters, *Chem.*
11 *Rev.*, 105, 3388-3431, doi:10.1021/cr040649c, 2005.

12 Deng, C., Zhuang, G., Huang, K., Li, J., Zhang, R., Wang, Q., Liu, T., Sun, Y., Guo, Z., Fu, J. S., and
13 Wang, Z.: Chemical characterization of aerosols at the summit of Mountain Tai in Central East China,
14 *Atmos. Chem. Phys.*, 11, 7319-7332, doi:10.5194/acp-11-7319-2011, 2011.

15 Desboeufs, K. V., Losno, R., and Colin, J. L.: Factors influencing aerosol solubility during cloud
16 processes, *Atmos. Environ.*, 35, 3529-3537, doi:10.1016/S1352-2310(00)00472-6, 2001.

17 Draxler, R. R., and Rolph, G. D.: HYSPLIT (HYbrid Single-Particle Lagrangian Integrated
18 Trajectory) Model access via NOAA ARL READY Website, available at:
19 <http://www.arl.noaa.gov/HYSPLIT.php> (last access: 1 February 2015), NOAA Air Resources
20 Laboratory, College Park, MD, 2014.

21 Fang, G. C., Huang, Y. L., and Huang, J. H.: Study of atmospheric metallic elements pollution in
22 Asia during 2000-2007, *J. Hazard. Mater.*, 180, 115-121, doi:10.1016/j.jhazmat.2010.03.120, 2010.

23 Fomba, K. W., Müller, K., van Pinxteren, D., and Herrmann, H.: Aerosol size-resolved trace metal
24 composition in remote northern tropical Atlantic marine environment: case study Cape Verde islands,
25 *Atmos. Chem. Phys.*, 13, 4801-4814, doi:10.5194/acp-13-4801-2013, 2013.

26 Gieré R., Blackford, M., and Smith, K.: TEM study of PM_{2.5} emitted from coal and tire
27 combustion in a thermal power station, *Environ. Sci. Technol.*, 40, 6235-6240, 2006.

28 Guo, J., Tilgner, A., Yeung, C., Wang, Z., Louie, P. K., Luk, C. W., Xu, Z., Yuan, C., Gao, Y., Poon,

1 S., Herrmann, H., Lee, S., Lam, K. S., and Wang, T.: Atmospheric peroxides in a polluted subtropical
2 environment: seasonal variation, sources and sinks, and importance of heterogeneous processes,
3 Environ. Sci. Technol., 48, 1443-1450, doi:10.1021/es403229x, 2014a.

4 Guo, L., Chen, Y., Wang, F., Meng, X., Xu, Z., and Zhuang, G.: Effects of Asian dust on the
5 atmospheric input of trace elements to the East China Sea, March Chem., 163, 19-27,
6 doi:10.1016/j.marchem.2014.04.003, 2014b.

7 Harris, E., Sinha, B., van Pinxteren, D., Tilgner, A., Fomba, K. W., Schneider, J., Roth, A., Gnauk, T.,
8 Fahlbusch, B., Mertes, S., Lee, T., Collett, J., Foley, S., Borrmann, S., Hoppe, P., and Herrmann, H.:
9 Enhanced role of transition metal ion catalysis during in-cloud oxidation of SO₂, Science, 340,
10 727-730, doi:10.1126/science.1230911, 2013.

11 Heal, M. R., Hibbs, L. R., Agius, R. M., and Beverland, I. J.: Total and water-soluble trace metal
12 content of urban background PM₁₀, PM_{2.5} and black smoke in Edinburgh, UK, Atmos. Environ., 39,
13 1417-1430, doi:10.1016/j.atmosenv.2004.11.026, 2005.

14 Hoek, G., Krishnan, R. M., Beelen, R., Peters, A., Ostro, B., Brunekreef, B., and Kaufman, J. D.:
15 Long-term air pollution exposure and cardio-respiratory mortality: a review, Environ. Health-Glob,
16 12, 43, doi:10.1186/1476-069X-12-43, 2013.

17 Hopke, P., Barrie, L., Li, S. M., Cheng, M. D., Li, C., and Xie, Y.: Possible sources and preferred
18 pathways for biogenic and non-sea-salt sulfur for the high Arctic, J. Geophys.Res.-Atmos., 100,
19 16595-16603, 1995.

20 Hsu, S.-C., Lin, F.-J., and Jeng, W.-L.: Seawater solubility of natural and anthropogenic metals
21 within ambient aerosols collected from Taiwan coastal sites, Atmos. Environ., 39, 3989-4001,
22 doi:10.1016/j.atmosenv.2005.03.033, 2005.

23 Hsu, S.-C., Wong, G. T. F., Gong, G.-C., Shiah, F.-K., Huang, Y.-T., Kao, S.-J., Tsai, F., Candice
24 Lung, S.-C., Lin, F.-J., Lin, I. I., Hung, C.-C., and Tseng, C.-M.: Sources, solubility, and dry
25 deposition of aerosol trace elements over the East China Sea, March Chem., 120, 116-127,
26 doi:10.1016/j.marchem.2008.10.003, 2010.

27 Hsu, S.-C., Lin, F.-J., Liu, T.-H., Lin, S.-H., Kao, S.-J., Tseng, C.-M., and Huang, C.-H.: Short time
28 dissolution kinetics of refractory elements Fe, Al, and Ti in Asian outflow-impacted marine aerosols

1 and implications, *Atmos. Environ.*, 79, 93-100, doi:10.1016/j.atmosenv.2013.06.037, 2013.

2 Hu, X., Zhang, Y., Ding, Z., Wang, T., Lian, H., Sun, Y., and Wu, J.: Bioaccessibility and health risk
3 of arsenic and heavy metals (Cd, Co, Cr, Cu, Ni, Pb, Zn and Mn) in TSP and PM_{2.5} in Nanjing,
4 China, *Atmos. Environ.*, 57, 146-152, <http://dx.doi.org/10.1016/j.atmosenv.2012.04.056>, 2012.

5 Husain, L., Ghauri, B., Yang, K., Khan, A. R., and Rattigan, O. V.: Application of the SO₄²⁻/Se
6 tracer technique to study SO₂ oxidation in cloud and fog on a time scale of minutes, *Chemosphere*,
7 54, 177-183, doi:10.1016/s0045-6535(03)00531-9, 2004.

8 Jakob, A., Stucki, S., and Kuhn, P.: Evaporation of Heavy Metals during the Heat Treatment of
9 Municipal Solid Waste Incinerator Fly Ash, *Environ. Sci. Technol.*, 29, 2429-2436,
10 doi:10.1021/es00009a040, 1995.

11 Jickells, T. D., An, Z. S., Andersen, K. K., Baker, A. R., Bergametti, G., Brooks, N., Cao, J. J., Boyd,
12 P. W., Duce, R. A., Hunter, K. A., Kawahata, H., Kubilay, N., laRoche, J., Liss, P. S., Mahowald, N.,
13 Prospero, J. M., Ridgwell, A. J., Tegen, I., and Torres, R.: Global iron connections between desert
14 dust, ocean biogeochemistry, and climate, *Science*, 308, 67-71, doi:10.1126/science.1105959, 2005.

15 Kaufman, Y. J., Tanré D., and Boucher, O.: A satellite view of aerosols in the climate system, *Nature*,
16 419, 215-223, 2002.

17 Li, W., Wang, Y., Collett, J. L., Jr., Chen, J., Zhang, X., Wang, Z., and Wang, W.: Microscopic
18 evaluation of trace metals in cloud droplets in an Acid precipitation region, *Environ. Sci. Technol.*,
19 47, 4172-4180, doi:10.1021/es304779t, 2013.

20 Li, W., Chi, J., Shi, Z., Wang, X., Chen, B., Wang, Y., Li, T., Chen, J., Zhang, D., Wang, Z., Shi, C.,
21 Liu, L., and Wang, W.: Composition and hygroscopicity of aerosol particles at Mt. Lu in South China:
22 Implications for acid precipitation, *Atmos. Environ.*, 94, 626-636,
23 doi:10.1016/j.atmosenv.2014.06.003, 2014.

24 Mackie, D. S., Peat, J. M., McTainsh, G. H., Boyd, P. W., and Hunter, K. A.: Soil abrasion and eolian
25 dust production: Implications for iron partitioning and solubility, *Geochem. Geophys. Geosyst.*, 7,
26 1-11, doi:10.1029/2006gc001404, 2006.

27 Mahowald, N.: Aerosol indirect effect on biogeochemical cycles and climate, *Science*, 334, 794-796,
28 doi:10.1126/science.1207374, 2011.

1 Moreno, T., Querol, X., Alastuey, A., Reche, C., Cusack, M., Amato, F., Pandolfi, M., Pey, J.,
2 Richard, A., Prévôt, A. S. H., Furger, M., and Gibbons, W.: Variations in time and space of trace
3 metal aerosol concentrations in urban areas and their surroundings, *Atmos. Chem. Phys.*, 11,
4 9415-9430, doi:10.5194/acp-11-9415-2011, 2011.

5 Newman, L.: Atmospheric oxidation of sulfur dioxide: A review as viewed from power plant and
6 smelter plume studies, *Atmos. Environ.* (1967), 15, 2231-2239, doi:10.1016/0004-6981(81)90255-9,
7 1981.

8 Oakes, M., Ingall, E. D., Lai, B., Shafer, M. M., Hays, M. D., Liu, Z. G., Russell, A. G., and Weber,
9 R. J.: Iron solubility related to particle sulfur content in source emission and ambient fine particles,
10 *Environ. Sci. Technol.*, 46, 6637-6644, doi:10.1021/es300701c, 2012.

11 Polissar, A. V., Hopke, P. K., and Harris, J. M.: Source regions for atmospheric aerosol measured at
12 Barrow, Alaska, *Environ. Sci. Technol.*, 35, 4214-4226, 2001.

13 Querol, X., Viana, M., Alastuey, A., Amato, F., Moreno, T., Castillo, S., Pey, J., de la Rosa, J.,
14 Sánchez de la Campa, A., Artíñano, B., Salvador, P., García Dos Santos, S., Fernández-Patier, R.,
15 Moreno-Grau, S., Negral, L., Minguillón, M. C., Monfort, E., Gil, J. I., Inza, A., Ortega, L. A.,
16 Santamaría, J. M., and Zabalza, J.: Source origin of trace elements in PM from regional background,
17 urban and industrial sites of Spain, *Atmos. Environ.*, 41, 7219-7231,
18 doi:10.1016/j.atmosenv.2007.05.022, 2007.

19 Quispe, D., Pérez-López, R., Silva, L. F. O., and Nieto, J. M.: Changes in mobility of hazardous
20 elements during coal combustion in Santa Catarina power plant (Brazil), *Fuel*, 94, 495-503,
21 <http://dx.doi.org/10.1016/j.fuel.2011.09.034>, 2012.

22 Reff, A., Bhawe, P., Simon, H., Pace, T. G., Pouliot, G. A., Mobley, J. D., and Houyoux, M.:
23 Emissions Inventory of PM_{2.5} Trace Elements across the United States, *Environ. Sci. Technol.*, 43,
24 5790-5796, doi:10.1021/es802930x, 2009.

25 Ren, L., Wang, W., Wang, Q., Yang, X., and Tang, D.: Comparison and trend study on acidity and
26 acidic buffering capacity of particulate matter in China, *Atmos. Environ.*, 45, 7503-7519,
27 doi:10.1016/j.atmosenv.2010.08.055, 2011.

28 Rubasinghege, G., Lentz, R. W., Scherer, M. M., and Grassian, V. H.: Simulated atmospheric

1 processing of iron oxyhydroxide minerals at low pH: roles of particle size and acid anion in iron
2 dissolution, *Proc. Natl. Acad. Sci. U.S.A.*, 107, 6628-6633, doi:10.1073/pnas.0910809107, 2010.

3 Schulz, M., Prospero, J. M., Baker, A. R., Dentener, F., Ickes, L., Liss, P. S., Mahowald, N. M.,
4 Nickovic, S., Garcia-Pando, C. P., Rodriguez, S., Sarin, M., Tegen, I., and Duce, R. A.: Atmospheric
5 transport and deposition of mineral dust to the ocean: implications for research needs, *Environ. Sci.*
6 *Technol.*, 46, 10390-10404, doi:10.1021/es300073u, 2012.

7 Schwab, J. J.: Aerosol chemical composition in New York state from integrated filter samples:
8 Urban/rural and seasonal contrasts, *J. Geophys. Res.*, 109, D16S05, doi:10.1029/2003jd004078,
9 2004.

10 Seinfeld, J. H., and Pandis, S. N.: *Atmospheric chemistry and physics: from air pollution to climate*
11 *change*, John Wiley & Sons, New Jersey, 2012.

12 Shafer, M. M., Perkins, D. A., Antkiewicz, D. S., Stone, E. A., Quraishi, T. A., and Schauer, J. J.:
13 Reactive oxygen species activity and chemical speciation of size-fractionated atmospheric particulate
14 matter from Lahore, Pakistan: an important role for transition metals, *J. Environ. Monit.*, 12, 704-715,
15 2010.

16 Shi, Z., Krom, M. D., Bonneville, S., Baker, A. R., Jickells, T. D., and Benning, L. G.: Formation of
17 iron nanoparticles and increase in iron reactivity in mineral dust during simulated cloud processing,
18 *Environ. Sci. Technol.*, 43, 6592-6596, 2009.

19 Solmon, F., Chuang, P. Y., Meskhidze, N., and Chen, Y.: Acidic processing of mineral dust iron by
20 anthropogenic compounds over the north Pacific Ocean, *J. Geophys. Res.*, 114, D02305,
21 doi:10.1029/2008jd010417, 2009.

22 Spokes, L. J., Jickells, T. D., and Lim, B.: Solubilisation of aerosol trace metals by cloud processing:
23 A laboratory study, *Geochim. Cosmochim. Acta*, 58, 3281-3287,
24 [http://dx.doi.org/10.1016/0016-7037\(94\)90056-6](http://dx.doi.org/10.1016/0016-7037(94)90056-6), 1994.

25 Takahashi, Y., Higashi, M., Furukawa, T., and Mitsunobu, S.: Change of iron species and iron
26 solubility in Asian dust during the long-range transport from western China to Japan, *Atmos. Chem.*
27 *Phys.*, 11, 11237-11252, doi:10.5194/acp-11-11237-2011, 2011.

28 Tian, H., Gao, J., Lu, L., Zhao, D., Cheng, K., and Qiu, P.: Temporal trends and spatial variation

1 characteristics of hazardous air pollutant emission inventory from municipal solid waste incineration
2 in China, *Environ. Sci. Technol.*, 46, 10364-10371, doi:10.1021/es302343s, 2012.

3 Tian, H., Liu, K., Zhou, J., Lu, L., Hao, J., Qiu, P., Gao, J., Zhu, C., Wang, K., and Hua, S.:
4 Atmospheric emission inventory of hazardous trace elements from China's coal-fired power
5 plants--temporal trends and spatial variation characteristics, *Environ. Sci. Technol.*, 48, 3575-3582,
6 doi:10.1021/es404730j, 2014.

7 Wang, Y., Zhang, X., and Draxler, R. R.: TrajStat: GIS-based software that uses various trajectory
8 statistical analysis methods to identify potential sources from long-term air pollution measurement
9 data, *Environ. Model. Soft.*, 24, 938-939, 2009.

10 Wei, F., Chen, J., Wu, Y., and Zheng, C.: Study of the background contents of 61 elements of soils in
11 China, *Environmental Science (in Chinese)*, 12 (4), 12-19, 1991.

12 Weichenthal, S., Villeneuve, P. J., Burnett, R. T., van Donkelaar, A., Martin, R. V., Jones, R. R.,
13 DellaValle, C. T., Sandler, D. P., Ward, M. H., and Hoppin, J. A.: Long-term exposure to fine
14 particulate matter: association with nonaccidental and cardiovascular mortality in the agricultural
15 health study cohort, *Environ. Health Perspect.*, 122, 609-615, doi:10.1289/ehp.1307277, 2014.

16 Wen, H., and Carignan, J.: Review on atmospheric selenium: Emissions, speciation and fate, *Atmos.*
17 *Environ.*, 41, 7151-7165, doi:10.1016/j.atmosenv.2007.07.035, 2007.

18 Werner, M. L., Nico, P. S., Marcus, M. A., and Anastasio, C.: Use of Micro-XANES to Speciate
19 Chromium in Airborne Fine Particles in the Sacramento Valley, *Environ. Sci. Technol.*, 41,
20 4919-4924, doi:10.1021/es070430q, 2007.

21 Xu, H. M., Cao, J. J., Ho, K. F., Ding, H., Han, Y. M., Wang, G. H., Chow, J. C., Watson, J. G., Khol,
22 S. D., Qiang, J., and Li, W. T.: Lead concentrations in fine particulate matter after the phasing out of
23 leaded gasoline in Xi'an, China, *Atmos. Environ.*, 46, 217-224, doi:10.1016/j.atmosenv.2011.09.078,
24 2012.

25 Yang, F., Tan, J., Zhao, Q., Du, Z., He, K., Ma, Y., Duan, F., Chen, G., and Zhao, Q.: Characteristics
26 of PM_{2.5} speciation in representative megacities and across China, *Atmos. Chem. Phys.*, 11,
27 5207-5219, doi:10.5194/acp-11-5207-2011, 2011.

28 Yang, Y., Wang, Y., Wen, T., Li, W., Zhao, Y., and Li, L.: Elemental composition of PM_{2.5} and PM₁₀

1 at Mount Gongga in China during 2006, Atmos. Res., 93, 801-810,
2 doi:10.1016/j.atmosres.2009.03.014, 2009a.
3 Yang, Y., Wang, Y., Wen, T., Zhao, Y., and Li, J.: Element Characterisitcs and Sources of PM2.5 at
4 Mount Dinghu in 2006, Environmental Science (in Chinese), 30, 988-992, 2009b.
5 Zhang, Q., Streets, D. G., Carmichael, G. R., He, K., Huo, H., Kannari, A., Klimont, Z., Park, I.,
6 Reddy, S., and Fu, J.: Asian emissions in 2006 for the NASA INTEX-B mission, Atmos. Chem.
7 Phys., 9, 5131-5153, 2009.

8

9

1 **Table 1.** Concentrations (mean \pm SD) of PM_{2.5} ($\mu\text{g m}^{-3}$) and trace elements (ng m⁻³) including total
2 and water soluble fraction at Mt. Lushan.

	Overall		Summer,2011		Spring,2012	
	Total	Water soluble	Total	Water soluble	Total	Water soluble
PM _{2.5}	55.2 \pm 20.1		55.9 \pm 21.8		54.7 \pm 18.9	
Al	449.1 \pm 441.1	73.3 \pm 93.5	369.1 \pm 464.4	108.0 \pm 121.7	515.1 \pm 415.2	48.9 \pm 57.3
Fe	331.1 \pm 236.2	71.5 \pm 70.5	330.4 \pm 250.9	101.9 \pm 70.5	331.6 \pm 227.3	15.7 \pm 12.9
Zn	258.3 \pm 162.8	172.9 \pm 105.8	274.3 \pm 129.5	211.9 \pm 104.4	245.3 \pm 186.1	142.3 \pm 97.5
Pb	68.2 \pm 49.3	29.4 \pm 23.8	65.4 \pm 47.3	37.8 \pm 27.5	70.5 \pm 51.4	22.7 \pm 18.3
Ba	63.8 \pm 54.2	23.4 \pm 17.0	66.0 \pm 71.1	19.3 \pm 15.0	61.9 \pm 33.6	26.7 \pm 18.0
Mn	22.2 \pm 12.2	15.5 \pm 8.1	24.7 \pm 12.5	19.0 \pm 8.8	20.2 \pm 11.6	12.8 \pm 6.3
As	21.5 \pm 19.6	14.8 \pm 11.9	22.3 \pm 16.3	12.4 \pm 6.1	20.9 \pm 22.2	17.0 \pm 15.1
Cr	13.7 \pm 17.2	0.7 \pm 0.5	18.2 \pm 19.5	0.8 \pm 0.6	9.6 \pm 13.8	0.3 \pm 0.1
Cu	12.4 \pm 9.6	9.9 \pm 8.9	13.2 \pm 6.4	10.7 \pm 6.9	11.7 \pm 11.6	9.3 \pm 10.2
Se	7.0 \pm 3.3	5.0 \pm 2.9	7.6 \pm 2.9	5.2 \pm 2.9	6.5 \pm 3.5	4.8 \pm 2.9
Cd	2.5 \pm 1.8	1.3 \pm 0.9	2.8 \pm 1.9	1.3 \pm 0.6	2.2 \pm 1.6	1.2 \pm 1.1
Mo	2.0 \pm 2.0	0.6 \pm 0.4	2.6 \pm 2.2	0.7 \pm 0.5	1.5 \pm 1.7	0.5 \pm 0.3

3

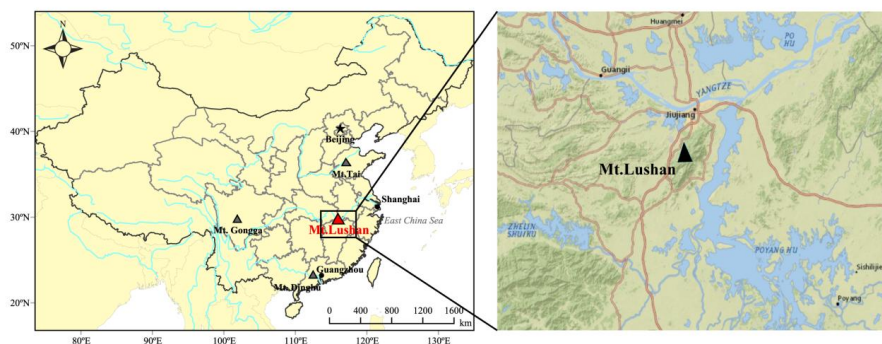


Figure 1. The location of Mt. Lushan and adjacent Yangtze River and Poyang Lake.

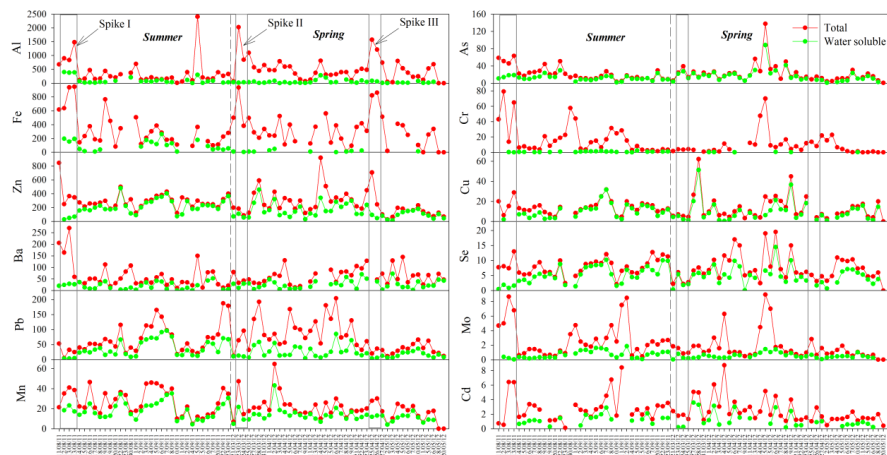
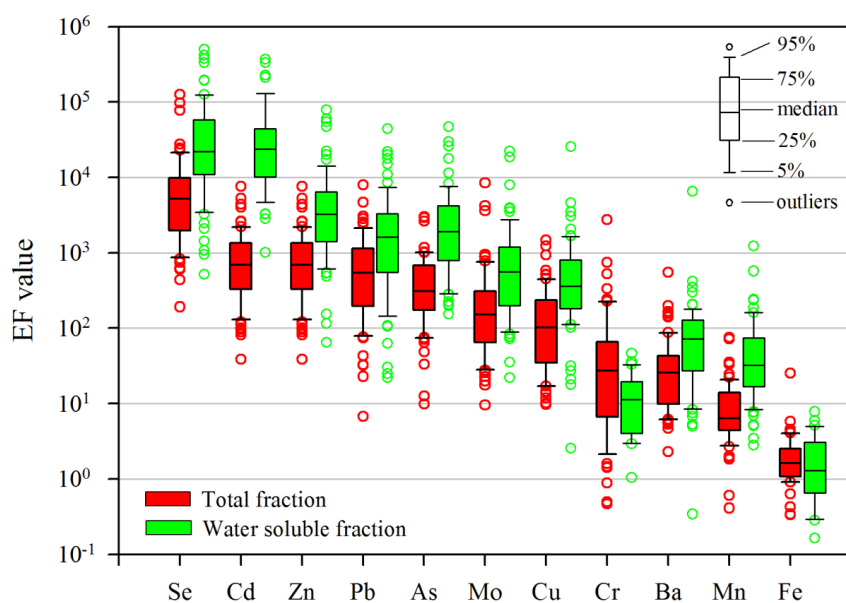


Figure 2. Temporal variations of individual trace element concentrations (ng m^{-3}) in $\text{PM}_{2.5}$ at Mt. Lushan. Boxes indicate the concentration spikes.

Comment [It16]: Add the unit of vertical axis in figure caption.



1
2 **Figure 3.** Enrichment factor (EF) values of fine particle trace elements at Mt. Lushan in total and
3 water soluble fraction.
4

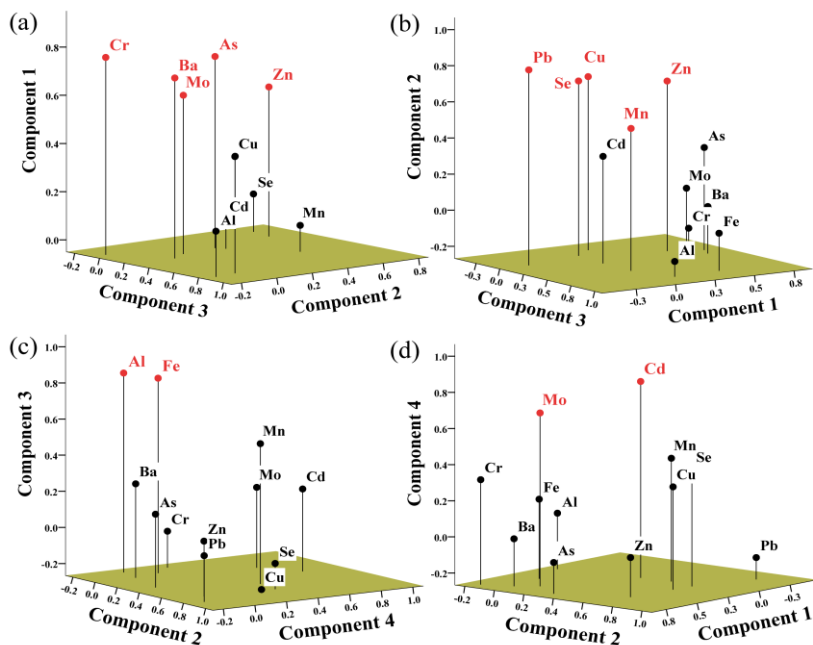


Figure 4. Loadings of (a) Component 1, (b) Component 2, (c) Component 3 and (d) Component 4 for trace elements in total fraction in PM_{2.5}.

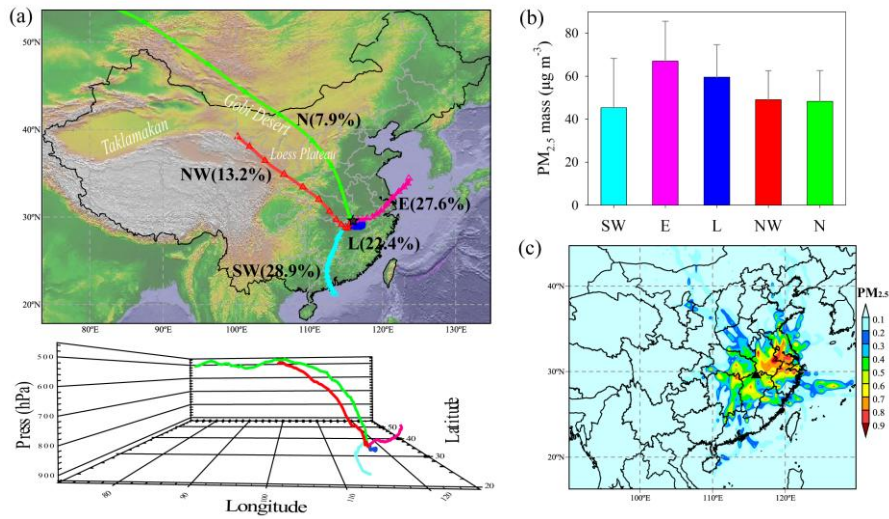


Figure 5. (a) Three-days mean trajectories arriving at Mt. Lushan, (b) averaged PM_{2.5} concentration of five clusters, and (c) the likely source regions of PM_{2.5} identified using PSCF plots during observation period.

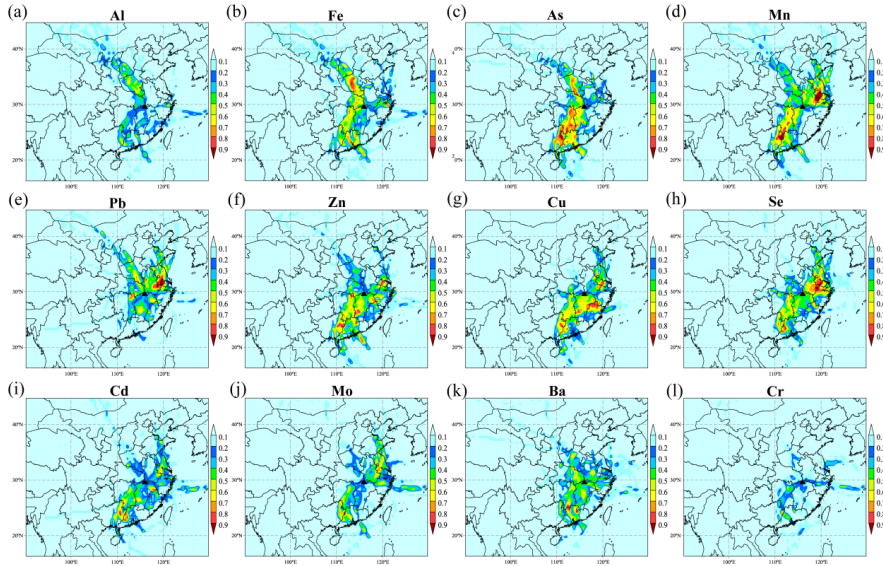
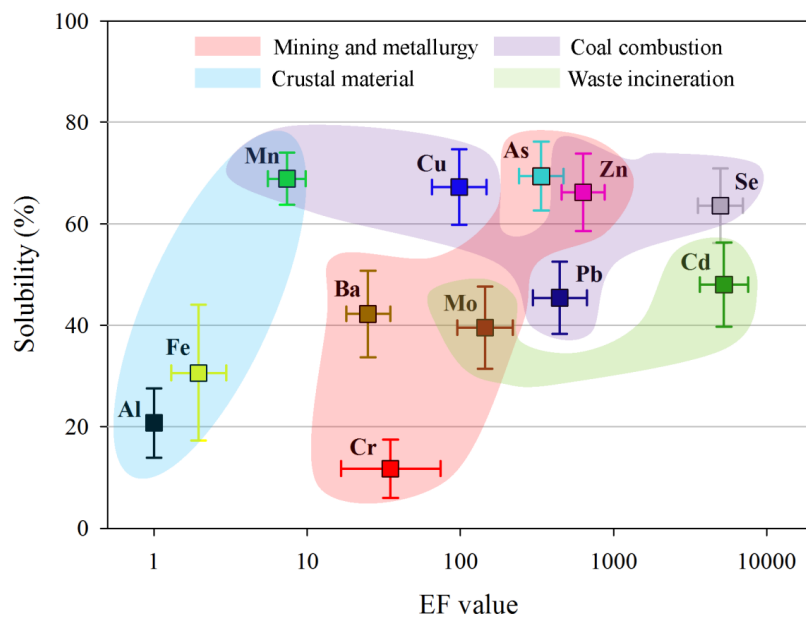


Figure 6. Likely source regions of individual elements in $PM_{2.5}$ at Mt. Lushan, identified using PSCF plots. Note the criteria are 75th percentile for Al and mean concentration for others.



1
2 **Figure 7.** Scatter plot of aerosol element solubility vs. logarithmic EF value, computed with
3 geometric mean in 99% confidence interval. Colored shade areas represent different sources
4 classified by EF value and PCA analysis.
5

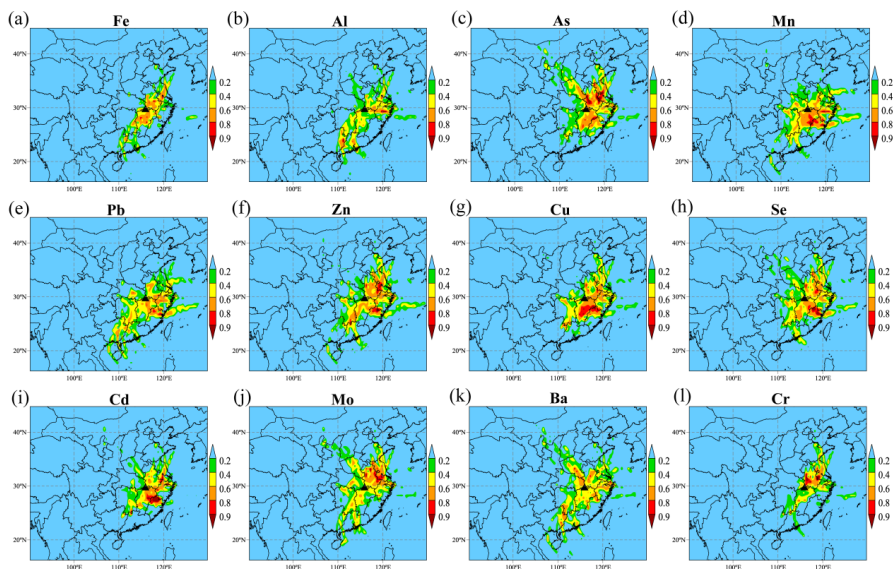
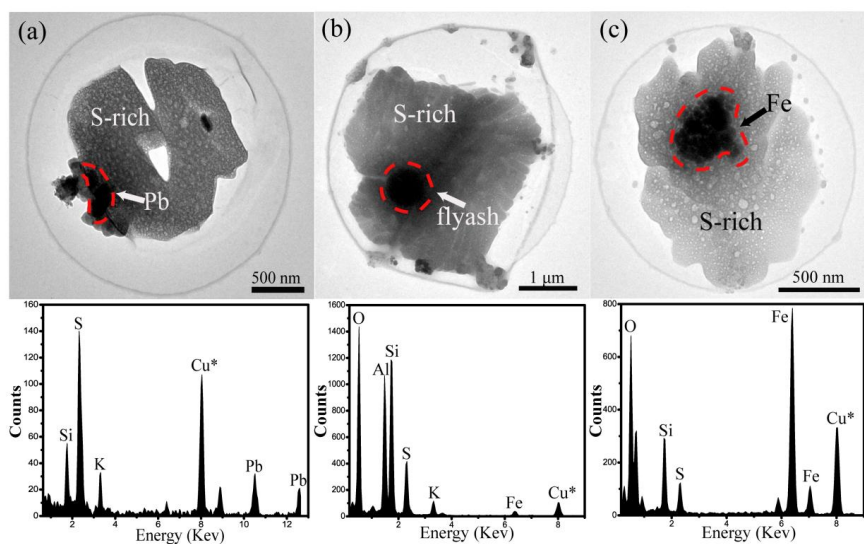


Figure 8. Solubility distributions in likely source regions for individual elements in $PM_{2.5}$ at Mt. Lushan, identified by PSCF with the mean solubility values as criteria.



1
2 **Figure 9.** Typical TEM images and corresponding EDS spectra of metal particles embedded in
3 individual S-rich cloud residues collected during cloud events. (a) Pb-S. (b) fly ash-S. (c) Fe-S. The
4 dotted red circles indicate the examined area of EDS. Cu* signals result from copper TEM grid.
5